MAGNETIC-FIELD ASSISTED FINISHING PROCESS (MAF) ON MOLD STEEL, CHROME-COATED SHEET METAL, AND ITS FUNDAMENTAL STUDY ON BRUSH CONSTITUENTS

By

Guangchao Song

A DISSERTATION

Submitted to
Michigan State University
in partial fulfillment of the requirements
for the degree of

Mechanical Engineering – Doctor of Philosophy

2023

ABSTRACT

Surface finishing is one of the most critical manufacturing processes as it improves the corrosion and fatigue resistance of a product. Among many available surface finishing technologies, Magnetic-Field Assisted Finishing (MAF) is a promising finishing process that uses a slurry mixture made of ferromagnetic and abrasive particles in a liquid medium, also known as a brush. The brush attached to a magnetic tool directly interacts with the surface of a workpiece and removes surface imperfections and defects to achieve a desired surface finish. The MAF process enables precise control of several parameters such as brush rotational speed, feed rate, gap distance, and the constituents of the MAF brush. These constituents encompass factors such as the size and type of abrasive and ferromagnetic particles. The control over the parameters allows for surface finishing to be precisely regulated down to the nanometer scale.

This research explores various aspects with the aim of improving the quality and processing time of the MAF process. Due to the recent inception of MAF, there is still a lack of understanding regarding the application of MAF on various metallic materials, large workpiece areas, and freeform geometries. In the first part of this study, a 2^{k-1} fractional factorial design (FFD) was used to investigate and identify optimal processing parameters on mold steels. The optimal processing parameters could be obtained by studying the interaction among all of the processing parameters. After the FFD, additional experiments were conducted to enhance the efficiency of the polishing process starting from a rough surface. Finally, a multi-step MAF process on the HP4M mold was designed based on the results obtained from both the FFD and additional experiments. The MAF performance was compared to manual finishing, where the final roughness of 26 nm and 20 nm were achieved with MAF and manual finishing, respectively, starting from the initial surface roughness of 434 nm. Additional experiments were conducted on an AISI S7 steel workpiece using

different processing parameters but employing the same analytical approach. The optimized parameter settings significantly improved the final surface roughness from 507 nm to 45 nm. Subsequently, the MAF process was employed to polish large chrome-coated sheet metal samples and the process was investigated to determine the optimal processing parameters. Based upon profilometry measurements, introducing a stiffer brush containing a greater fraction of ferromagnetic particles by weight improved the MAF performance in finishing sheet metal samples. Additionally, using the smallest black ceramic (BC) size (3 μm) resulted in a superior surface finish.

The second part of the study was closely related to the previous study but focused on the finishing of large sheet-metal surfaces. First, the optimal processing parameters were determined by applying a small-scale setup to finish chrome-coated metal sheet samples. Subsequently, the identified parameters were implemented in the continuous setup that successfully finished the sheet metal samples with a larger area. This application of optimized parameters in the continuous setup enhances the effectiveness and efficiency of the overall finishing process.

Finally, a systematic approach was developed to identify the optimal processing conditions regarding the abrasive particle size, iron particle size, and traversing passes. The study yielded the appropriate brush constituents to improve the efficiency of the MAF process. To enhance material removal and improve the surface quality of the workpiece, it is recommended to use smaller BC polishing media and larger iron particle sizes. The optimal number of passes varied depending on the size of the BC. As the BC size decreased, optimal conditions required fewer passes, resulting in a better surface finish. Simulations were conducted to explore the effects of the iron particle size on the brush constituents. The investigations demonstrated that the larger iron particles are subject to a more powerful magnetic force. As a result, they form robust chain-like structures that exhibit

a two-body abrasion mechanism, providing enhanced processing capability. Conversely, the smaller iron particles experience comparatively weaker magnetic forces between them, enabling them to roll freely, resulting in a three-body abrasion mechanism. The current status of the MAF process is still not mature enough to be implemented in practical industrial applications, but his work determined the optimal contents of the brush constituents which will contribute to making the MAF process more practical.

To my dearest and loving parents.
Thank you for always believing in me.

ACKNOWLEDGEMENTS

I extend my heartfelt gratitude to my academic advisor, Dr. Patrick Kwon. When I first joined his program as a graduate student, the idea of pursuing a Ph.D. never crossed my mind. However, with his warm introduction and steadfast guidance, I entered his lab and embarked on the journey toward a Ph.D. His mentorship has been my guiding light, consistently steering me in the right direction while offering unwavering support both academically and personally. None of my accomplishments would have been possible without his invaluable guidance and trust. Thank you immensely for your guidance and belief in me. I also wish to express my sincere appreciation to Dr. Haseung Chung for his continuous expertise and insightful suggestions throughout my studies. His feedback during our group meetings consistently motivated and enlightened me. I extend my gratitude to Dr. Guo Yang and Dr. Thomas Bieler for their invaluable feedback and comments on my dissertation and ongoing projects.

My gratitude extends to my colleagues and collaborators who have provided boundless support in my academic and emotional journey. A special thanks to Bibek Poudel, my fellow lab colleague and friend, whose suggestions always spurred me to view my studies and work from different angles. I also extend my thanks to Hawke Suen, Zhiyuan Qu, Hoa Nguyen, Jisheng Chen, Dr. Pil-ho Lee, Dr. Himanshu Saharshabudhe, and all the colleagues, advisors, and professors who bolstered my research endeavors. I would also like to thank my parents and family. Their unwavering financial and emotional support, along with their unshakeable belief in me, have been the foundation of my persistence. Lastly, I am deeply grateful to my girlfriend, Serena Lyu. Her unwavering belief in me and the warmth she provides, akin to that of a family member, have been my pillars of strength. Thank you for your love, patience, guidance, and unending support. My journey to success would not have been possible without you all.

TABLE OF CONTENTS

CHAPTER 1: INTRODUCTION 1

CHAPTER 2: INVESTIGATION OF OPTIMAL PROCESSING PARAMETERS FOR DIFFERENT METALS BY MAF PROCESS 16

CHAPTER 3: CONTINUOUS SETUP FOR THE LARGE AREA FINISHING BY MAF PROCESS 41

CHAPTER 4: FUNDAMENTAL STUDY ON MAF BRUSH CONSTITUENTS 48

CHAPTER 5: SUMMARY AND FUTURE WORK 64

BIBLIOGRAPHY 67

CHAPTER 1: INTRODUCTION

1.1 Background

1.1.1 Surface Finishing

Surface finishing is one of the most crucial procedures in manufacturing processes as it influences the aesthetic appearance and mechanical or chemical behavior of a manufactured product. It also determines how the manufactured part interacts with other parts in contact interfaces. Surface finishing processes encompass a wide array of industrial techniques that involve the addition, removal, or reshaping of manufactured parts to achieve a desired surface quality for many applications in aerospace, biomedical tools and orthopedic implants, the mold industry, and so on. In surface finishing, the foremost important action is to remove the undesired surface irregularities. Achieving an appropriate surface finish is vital for enhancing the appearance and durability of the product. The surface of a finished part typically exhibits a multitude of characteristics, including varying levels of roughness and an assortment of defects that encompass features such as uneven surfaces, fractured edges, burrs, scratches, micro-cracks, and other irregularities. These unwanted defects impact not only the quality and usability of the manufactured component in its wear, corrosion, and fatigue resistance, but also the entire machine assembly accuracy, serviceable performance, and life after the assembly of a part [1].

One of the notable impacts of surface finishing is on corrosion resistance which is the ability of a material to withstand the damaging effects of corrosion, which is the gradual deterioration or destruction of a material due to chemical reactions with its environment. Metal with a better surface finish improves the corrosion resistance to enhance the performance and service life [2]. The most important benefit of surface finishing is the improvement of fatigue life. Metal parts must withstand mechanical stress and corrosion for long-term use. Some surface anomalies, such as burs and metal lines which are formed from machining, can lead to premature failure [3, 4]. By removing those imperfections on the surface of a metal part, the fatigue life of the part will be greatly improved. Furthermore, the durability and wear resistance of the component is intricately linked to the surface roughness. Bayer [5] reported that wear increased with the increasing roughness of the surface and was more sensitive to surface roughness variations for finer surfaces. Consequently, the surface qualities of components yield substantial repercussions, influencing not only their usability, longevity, and dependability but also establishing an interconnection with the overall performance and lifespan of the machinery. Overall, surface finishing technology is one of

the key methods to enhance serviceable performance, increase reliability, and prolong the service life of the parts and products.

1.1.2 Surface Texture

Surface texture is the repetitive or random deviation from the nominal surface that forms the three-dimensional topography of the surface. Surface texture includes roughness, waviness, lay, and flaws, as shown in Figure 1.1.

The determination of surface roughness involves the examination of short-wavelength fluctuations characterized by the presence of hills (asperities or local maxima) and valleys (local minima) exhibiting varying amplitudes and spacings. On the other hand, waviness pertains to longer-wavelength irregularities, known as macro-roughness, which may arise due to various factors such as machine or workpiece deflections, vibrations, chatter, and heat treatment [6]. Furthermore, surface lay denotes the primary direction of the prevailing surface pattern, which is inherently influenced by the specific production method employed. Lastly, flaws represent unintended and undesirable disruptions within the surface texture.

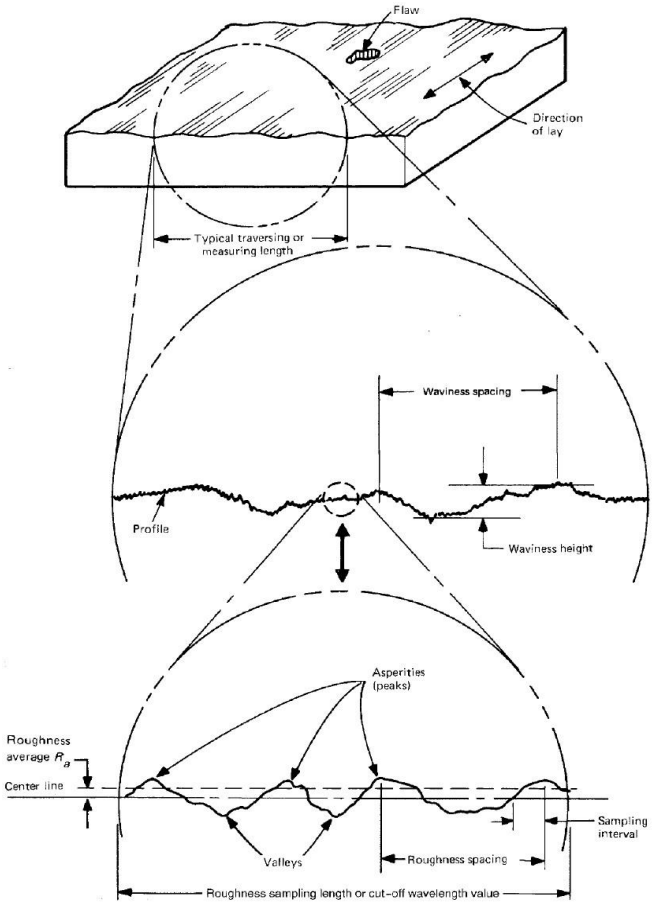

Figure 1.1: Pictorial display of surface texture [6]

1.1.3 Surface Roughness

Surface finish evaluation can be effectively accomplished by scrutinizing the surface roughness parameters, as they constitute the foremost indicators for characterizing surface topography. Surface roughness is used to measure the vertical characteristics of the surface deviations [7]. There are two parameters commonly used:

R_a, the arithmetic average height parameter, also known as the central or mean line average, is the most universally used roughness parameter for general surface quality control. It is defined as the average absolute deviation of the roughness irregularities from the mean line over one sampling length as shown in Figure 1.2 [7]. The mean line serves as a reference point, ensuring that the area enclosed between the profile and the mean line above matches the area below it.

The mathematical definition of the arithmetic average height parameter is as follows:

$$R_a = \frac{1}{L}\int_0^L |z|\, dx$$

where z is the profile height, and L is the evaluation length.

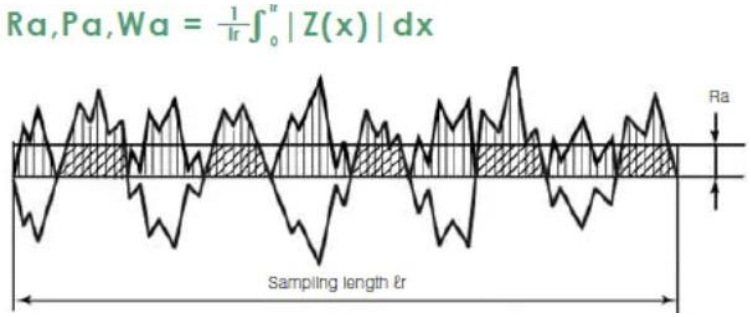

Figure 1.2: Arithmetic mean height for roughness profile (R_a) [8]

R_z, the average value of the heights of the five highest-profile peaks and the depths of the five deepest valleys within the evaluation length, as shown in Figure 1.3. This parameter is more sensitive to occasional high peaks or deep valleys than R_a.

The mathematical definition of the arithmetic average height parameter is as follows:

$$R_z = \sum_{i=1}^{5} \frac{P_i - V_i}{5}$$

where P_i is the highest peak, and V_i is the lowest valley.

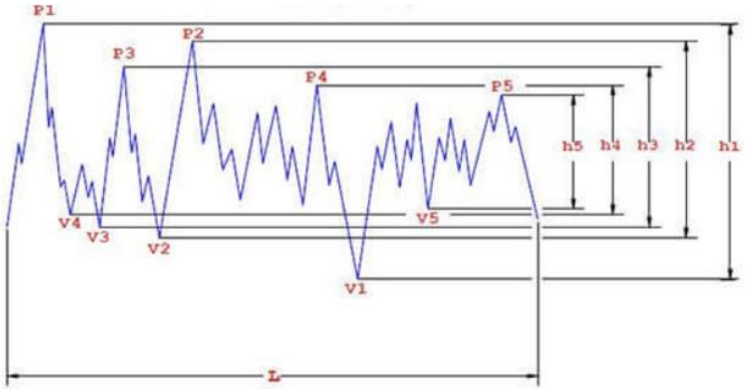

Figure 1.3: Average value of five heights between max & min (R_z) [9]

1.2 Surface Finishing Technologies

1.2.1 State of the Art

To ensure and optimize the quality of the surface, it is imperative to employ the most effective method of superfine finishing. There are varieties of processing methods for implementing the finishing technology which can be classified by supplied energy in the finishing process that includes mechanical method, chemical and electrochemical method, and heat energy method according to Yang et al. [1]. A classification of surface finishing techniques is in Figure 1.4.

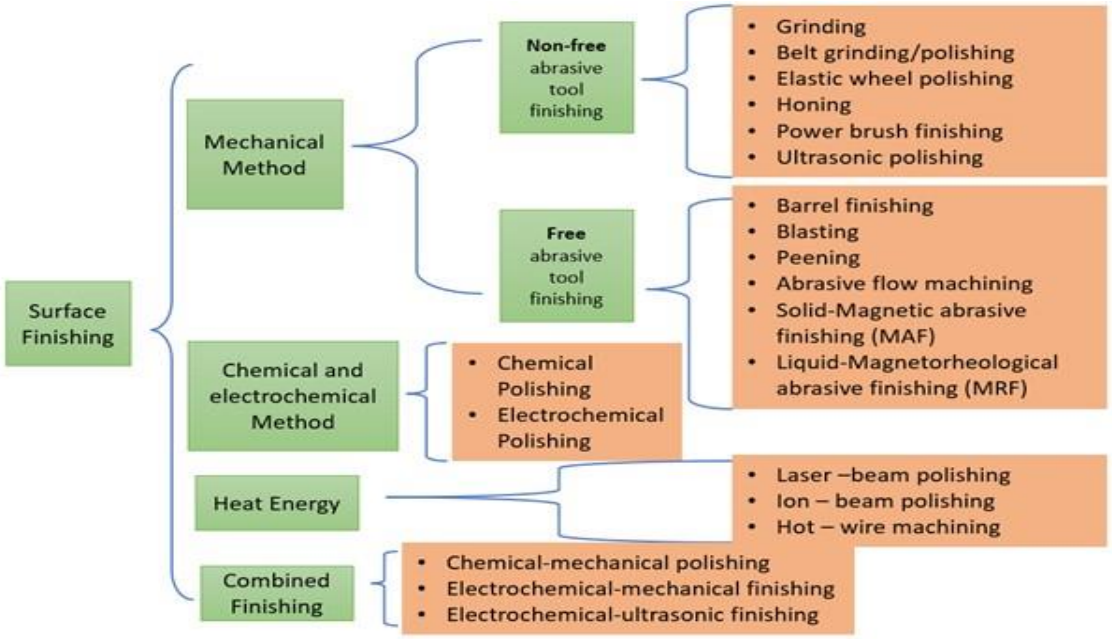

Figure 1.4: Classifications of surface finishing techniques

In the mechanical method, two categories can be classified based on the state of the abrasive [10]. The first one is called bonded abrasive state or non-free abrasive tool finishing, in which the abrasives are embedded in a substrate matrix such as polymer core, cloth, plastic film, and so on.

The non-free abrasive tools include abrasive stones, coated abrasives, and abrasive media. Examples of abrasive stones are grinding plates and honing tools [11]. Coated abrasives are composed of abrasives bonded to a flexible substrate such as sandpaper or belt. Abrasive media consists of abrasives bonded to a polymer core, and it is widely used for a variety of shape polishing including spheres, cones, triangles, ellipses, etc. to achieve a mass finishing process.

The other category in the mechanical finishing method is called unbonded abrasive state or free abrasive tool finishing, where abrasives freely participate in the finishing process. They are in a loose state during the finishing process, working on the surface of the workpiece with varying speed and pressure to improve surface quality. Free abrasive finishing technology includes shot peening, abrasive flow machining (AFM), magnetic abrasive finishing (MAF), magnetorheological fluid finishing (MRF), and so on. Shot peening is a cold work process used to impart compressive residual stresses onto the surface of a component, which results in modified mechanical properties [12]. AFM finds predominant utility in the domain of internal tube finishing, introducing a semi-solid abrasive medium flowing in the channel of the workpiece by relatively high pressure, to remove burrs and surface irregularities of the workpiece channel [13]. MAF is another free abrasive finishing method with a brush composed of ferromagnetic and abrasive particles. Abrasive particles can be embedded or integrated with the ferromagnetic matrix particle, and it forms a semi-solid brush under a magnetic field. The use of alternating magnetic fields in the MAF process has successfully attracted industrial applications such as surface and edge finishing and deburring of intricate components. Similarly, MRF is comparable with MAF, however, a liquid medium is introduced into the ferromagnetic and abrasive particles so that the brush becomes a Newtonian fluid without the presence of a magnetic field but with enhanced brush performance such as stiffness and shear yield strength in the presence of the magnetic field. Both of these methods are sub-categories under magnetic field assisted finishing (MAF), which initiate the finishing applications on optics as a flexible abrasive tool that could easily accommodate the freeform surface of the workpiece, and lead to a nano-scaled surface finish [14].

Chemical and electrochemical polishing are considered for surface finishing additive manufactured components. This method requires less tooling than mechanical polishing. The anode is commonly referred to as a workpiece and the cathode are immersed in an electrolyte solution. Then, a DC power is introduced to supply the current to the electrodes to initiate the polishing process [15]. The advantage of this process is that it can remove the surface irregularities

of intricate surfaces. However, it also has potential risks to human health due to the hazardous chemicals.

Another efficient, accurate, and fast surface finishing method is thermal finishing. In this method, a laser or ion beam is projected onto the surface, providing thermal energy to the target surface. Laser finishing does not remove material from the surface, instead redistributes the material through melting and re-solidification. Zhou et al. [16] demonstrated laser polishing on additive manufacturing Ti-6Al-4V and reported roughness reduction up to 1 μm. However, this surface-finishing technology consumes significant amounts of energy compared to other surface-finishing techniques.

1.3 Motivations

Considering hazardous risks and tremendous energy consumption by using chemical and electrochemical finishing techniques and thermal energy finishing methods, respectively, the mechanical finishing method is preferred as a safer and lower-cost way to achieve superfine finishing on manufactured products. Nevertheless, within the domain of mechanical superfine finishing, there exist numerous finishing methods that necessitate thorough evaluation and scrutiny. To determine an appropriate mechanical fine-finishing method, several criteria should be considered:

Final desired roughness: The selection of a proper method among different surface finishing techniques has a significant impact on achievable final roughness, as shown in Figure. 1.5 [10]. For instance, if the desired final roughness needs to be around nano-level scaled, buffing, polishing, or magnetic abrasive finishing can be selected since their attainable surface roughness is below a hundred nanometers.

Process		Ra μm
Base	Grinding	0.3~0.8
	Hard turning	0.2~1.0
Abrasive fine-finishing	Stone superfinishing	0.05~0.15
	Tape superfinishing	0.05~0.2
	Honing	0.25~0.5
	Mass finishing	0.05~0.1
	Lapping	0.05~0.12
	Polishing	0.01~0.05
	Buffing	0.005~0.01
	Abrasive flow machining	0.1~0.25
	Magnetic abrasive finishing	0.003~0.07

Figure 1.5: Characteristics of surfaces created by typical abrasive fine-finishing methods

Better controllability: by adjusting the parameters involved in the finishing process such as abrasive size, tool working speed, etc., the material removal rate and final surface roughness can be controlled.

Simplicity in processing equipment: only general equipment (CNC milling) is needed to finish the surface.

Strong adaptability to freeform surfaces: the chosen method should accommodate the shape of the workpiece such as using a flexible finishing tool.

By employing such screening criteria, one can effectively identify a suitable method for achieving a superfine finishing outcome. Those methods that cannot achieve superfine finishing on intricate surfaces are excluded such as grinding, honing, massive finishing, etc. Eventually, the MAF process met all requirements as it has relatively high material removal and achievable surface roughness at the nano-scaled level [17], and the flexible tool brush allows freeform geometries to remove surface irregularities. The shape of the brush is not a huge concern as the MAF brush can dynamically adapt to the surfaces of the workpiece. By adjusting the brush composition or magnetic field intensity, the material removal rate and final surface roughness can be manipulated, satisfying the criteria of better controllability. Furthermore, MAF is compatible with the standard CNC milling machine which makes the automation and easier setup for the surface finishing process.

1.4 MAF

1.4.1 Introduction

As stated earlier, magnetorheological finishing (MRF) is one of the sub-categories of magnetic-field assisted finishing (MAF). Magnetorheological (MR) fluid is a new smart material developed by Rabinow in 1949 [18]. It is a viscous suspension prepared by dispersing the ferromagnetic particles in a carrier fluid. MR fluid is a free-flowing liquid with all properties of the Newtonian fluid without a magnetic field. However, when an external magnetic field is applied near the MR fluid, the rheological properties of the MR fluid will change dramatically due to the ferromagnetic dipoles attracting to each other and forming a chain-like structure along the direction of the magnetic field, as shown in Figure 1.6[1]. Thus, it increases the viscosity and shear yield stress in such a medium.

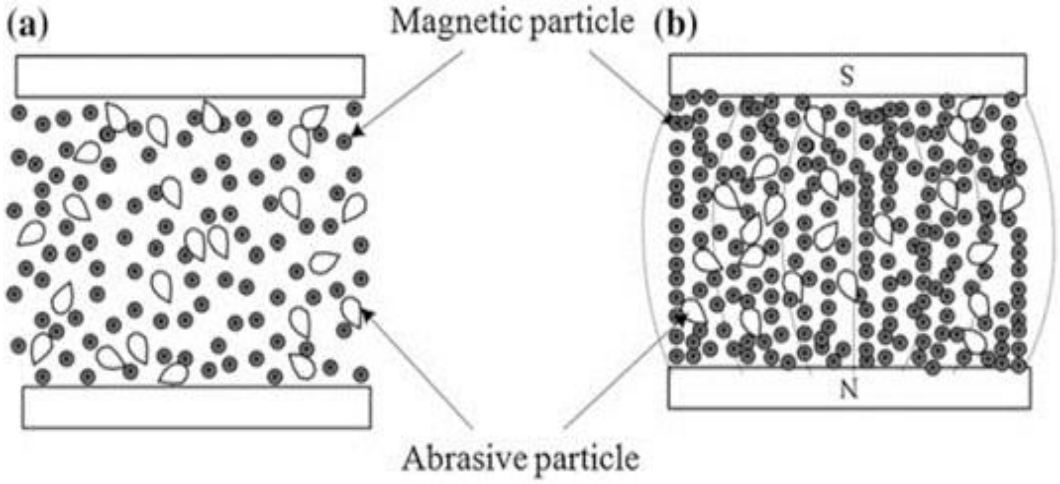

Figure 1.6: Schematic diagram of the microscopic structure of MR fluid without and with external magnetic force

In the MAF process, with the unique property of MR fluid, abrasive is introduced to form a flexible finishing brush. This brush can be attached to a magnetic tool directly interacting with the surface of a workpiece. During the tool's traversal movement across the surface, the translation and rotation motions of the brush, particularly the abrasive particles within it, effectively eradicate minute quantities of material from the surface. This meticulous process serves to eliminate surface imperfections and enhance overall surface quality as the process continues. One notable advantage of MAF is its seamless integration into computer numerical control (CNC) milling machines, facilitating a streamlined operational process, as shown in Figure 1.7. In addition, some other additives such as exfoliated graphene nanoplatelets (xGnPs), working as a nanoscale

solid lubricant, can be introduced into the finishing brush to improve the brush performance and prolong the MAF brush life [19].

Figure 1.7: CNC Setup with attached magnetic tool holder

1.4.2 State of the Art

Experimental setup: The MAF, specifically referred to as MRF, has three critical methodologies which are explored in the literature: (a) rotating wheel, (b) rotating tool, and (c) rotating disk [20], as shown in Figure 1.8.

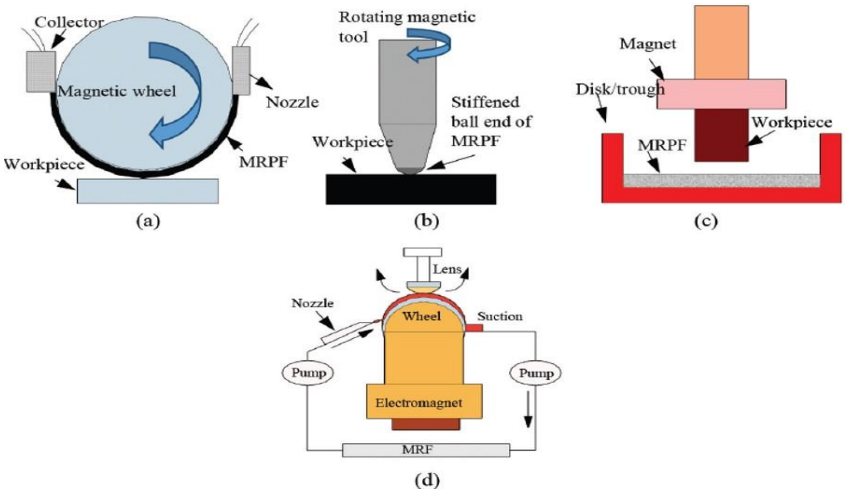

Figure 1.8: Schematic of different finishing methods in the MAF process

In the rotating wheel method shown in Figure 1.8 (a), a carrier wheel with magnetic material is rotating. During the process, a limited thickness of the MAF medium is added onto the wheel, and due to the magnetic field of the wheel, the ribbon of the MAF medium becomes stiff in the polishing zone. Because of a gradient in the magnetic field, ferromagnetic particles move toward the wheel, and abrasive particles approach the flat area of the workpiece. This setup is used to finish aspheric components such as an aspheric lens in optics [21]. Another experimental arrangement of the rotating wheel method for spherical lens finishing is shown in Figure 1.8 (d). This configuration is the extension of the rotating wheel method. The spherical lens rotates about the spindle (Z-axis), and the spindle also swings at a precise angle so that the utilization of a magnetic abrasive brush facilitates the attainment of a uniformly finished surface on a spherical lens.

In the rotating tool method [22, 23], the MAF medium is attached to the end of a magnetic finishing tool, which produces a flexible finishing pad. The revolving polishing device also called the ball end MAF, can finish complex surfaces such as convex, concave, sphere, and even freeform. The finishing mechanism of this ball-end MAF method is shown in Figure 1.8 (b). Since it is a relatively new technology and its initial purpose is for polishing optical components, some researchers attempted to utilize MAF on other materials. Miao et al. [24] found the normal force and shear stress increase with the addition of either abrasive or deionized water (DI) water on aluminum oxynitride material. Sidpara and Jain [25] reported the final Ra was highly influenced by Carbonyl Iron Particles (CIPs) concentration and was slightly influenced by the initial surface roughness value on the single-crystal silicon. Kumar et al. [26] investigated the MAF on Polylactic acid (PLA) material and the surface roughness eventually achieved 81 nm in 75 minutes. Furthermore, other researchers dedicated their studies to finish the surface of metallic alloys. Parameswari et al. [27] found that as abrasive particle concentration and wheel speed increased, the change in both surface roughness and finishing rate was increased by using the rotating wheel method of MAF on the Ti-6Al-4V disc. The minimum Ra of 28.8 nm was achieved via MAF on a rectangular disk of copper alloy reported by Kansal et al. [28] since copper is one of the softer metals. It can be observed that most MAF processes are applied to non-metallic material. Despite the use of the MAF processes for metal finishing, the finishing technique is constrained using a rotating wheel; however, it is challenging to finish the complex freeform surface geometry.

Processing parameters or variables also affect the MAF performance because they influence the properties of the MAF brush. MAF performance is measured by the finishing efficiency and the quality of the final surface. The finishing efficiency describes the material removal rate during the finishing process, and the final surface roughness value is the index of final surface quality. These indicators are affected by many parameters as follows:

Conditions of the MAF brush composition tremendously influence MAF performance, and those conditions can include the type and size of abrasive, volume fraction of ferromagnetic particles, and other additives in the brush.

The choice of abrasive type needs to be correlated with the physical and mechanical properties of the workpiece. In the MAF process, the most commonly used abrasive material is the compound called silicon carbide (SiC), composed of silicon (Si) and carbon (C). SiC has high hardness but is inherently brittle. The hardness of the SiC abrasive, also known as black ceramic (BC), is higher than the corundum abrasives. Thus, SiC abrasive can be widely used in MAF brushes. It should be noted that in the conventional grinding process, SiC could have a strong chemical reaction with steel material because SiC is a highly thermally conductive material and the high temperature generated in the grinding process leads to the formation of intermetallic compounds between silicon, carbon, and iron. In the MAF process, due to the good heat dissipation of the MAF brush, the processing temperature is not too high [1]. Thus, SiC is one of the most appropriate choices in the MAF process. The selection of abrasive particle size predominantly relies on considerations of finishing efficiency and desired surface roughness outcomes. A finer size should be considered when a finer surface roughness on a workpiece is required but the material removal rate is lower. If the initial roughness of the workpiece surface is rougher, the coarse abrasive should be chosen to obtain a higher material removal rate and eventually this must be followed with the fine finishing process.

The material removal rate in the MAF process is directly influenced by the volumetric percentage of abrasive material present in the MAF brush. Generally, abrasive particles with higher volume fraction seem to have higher finishing (or grinding) efficiency. In the MAF process, however, assuming that the total volume of the MAF brush stays constant, increasing the volume fraction of abrasive particles will reduce the volume of ferromagnetic particles. The volume fraction of the ferromagnetic particles determines the stiffness of the MAF brush due to the number of chain-like structures presented in the brush, which influences the shear yield strength of the brush.

Another factor with a huge impact on the shear yield strength of the MAF brush is magnetic field strength. A higher magnetic field strength provides higher grinding pressure and shear stress due to the higher stiffness of the MAF brush, yielding a better finishing efficiency, but it can also deteriorate the surface finishing due to excessive grinding. Consequently, during the initial roughing stage, it is advisable to employ a higher magnetic field strength to amplify the material removal rate. In subsequent stages, the magnetic field strength should be gradually reduced to attain a finer surface roughness.

Other factors also play important roles in the MAF process. The rotational speed and feed rate of the brush tool could affect the MAF efficiency due to the related shear rate. The gap distance between the magnet and the workpiece influences the magnetic field strength during the MAF process.

To obtain a better result in MAF performance, many researchers adopted the design of experiment (DOE) method and statistical analysis to carry out the optimal processing parameters for the MAF study. Khan et al. [29] used a three-level factorial design, finding that abrasive size is the most important parameter followed by iron powder concentration and abrasive concentration. Pan et al. [30] studied MAF fluid and processing parameters in the MAF process with a dynamic magnetic field for a sapphire workpiece. They chose four factors, including gap distance, polishing disc speed, magnetic pole speed, and workpiece speed, and three levels of orthogonal experiments to determine the optimal processing parameters. Singh [31] found the most dominant factor was applied voltage followed by the working gap; however, the effects of abrasive powder mesh number and rotational speed seemed to be very small. By using a ball end MAF, Saraswathamma [32] used DOE analysis on silicon and carried out the result of that working gap was found to be the critical process parameter for silicon. It can be also seen from other researchers' work on finding the optimal processing parameters in the MAF process[23, 33–35]. Thus, the methodology of using the DOE and statistical analysis is critical to compare the effect and dependence among the processing parameters.

Achievement in MAF for applying to freeform surfaces: Freeform surfaces are widely used in the medical, aerospace, and automobile sectors. The primary purpose of the MAF process is to implement it in 3D freeform geometries finishing. As mentioned previously, the remarkable adaptability of the MAF brush stems from its ability to automatically conform to the workpiece surface. This is achieved through the formation of a flexible grinding layer that interacts with the

contact surface. Even if the chain-like structures of ferromagnetic particles experience disruption during the finishing process due to the dynamic motion of the workpiece, they promptly reassemble under the influence of an external magnetic field. In essence, the MAF brush dynamically adjusts to the contours of the workpiece surface, ensuring optimal adaptability. Therefore, a continuous finishing process on the freeform surface of the workpiece with irregular shapes will be achieved by using the MAF process. It is beneficial to the aerospace and medical industry as the MAF process is capable of giving nano-scaled surface finishing on complicated geometries or difficult-to-approach regions of the component.

There are many topics and experiments to investigate the application of the MAF process on 3D freeform surfaces. Barman and Das [36] designed and fabricated a novel polishing tool for finishing freeform surfaces in the MAF process. Mu-metal (Ni-Fe Alloy) was chosen as a material for the magnet holder due to its excellent magnetic field shielding property. The analysis of forces acting on the workpiece during the MAF process is also critical as it is crucial in the understanding of the workpiece-abrasive particles interaction in the finishing process. Sidpara and Jain [37] achieved such force analysis on a replica of a knee joint implant, and they claimed that the theoretical normal force, as well as the tangential force, is less than those of experimental forces in the case of the angle of curvature of the workpiece surface. In 2012, the same group examined nano finishing of freeform surfaces of prosthetic knee joint implants. In this instance, an optimal quantity of chemicals (HF and HNO3) was introduced into the MAF brush, resulting in a notable enhancement of the processing time, even in the presence of considerable initial surface roughness [25]. Another research group experimented on different projection angles of freeform for the MAF process [38], and found that the surface roughness was reduced substantially when the projection angle approached zero degrees, which meant that the MAF process would perform the best when polishing flat samples.

It is also a challenge by using a two-and-half or three-axis CNC milling machine during the MAF process for the freeform surface finishing because even though the MAF brush can adapt to the different shapes of the surface, the magnetic field generated from the magnet is always aligned with the direction of the tool holder. In other words, the magnetic field in which the field lines are normal to the tangential surface of the freeform will provide the strongest magnetic field during MAF finishing on the complicated geometry. Alam et al. [39] developed a customized five-axis CNC controller to provide a fully automated freeform surface finishing, and they finally obtained

a uniform finish on the workpiece. In contrast, Yamaguchi and Graziano [40] designed a knee holder which was compatible with a robot arm so that the knee component could be placed and orientated at different angles with respect to a stationary brush as shown in Figure 1.9.

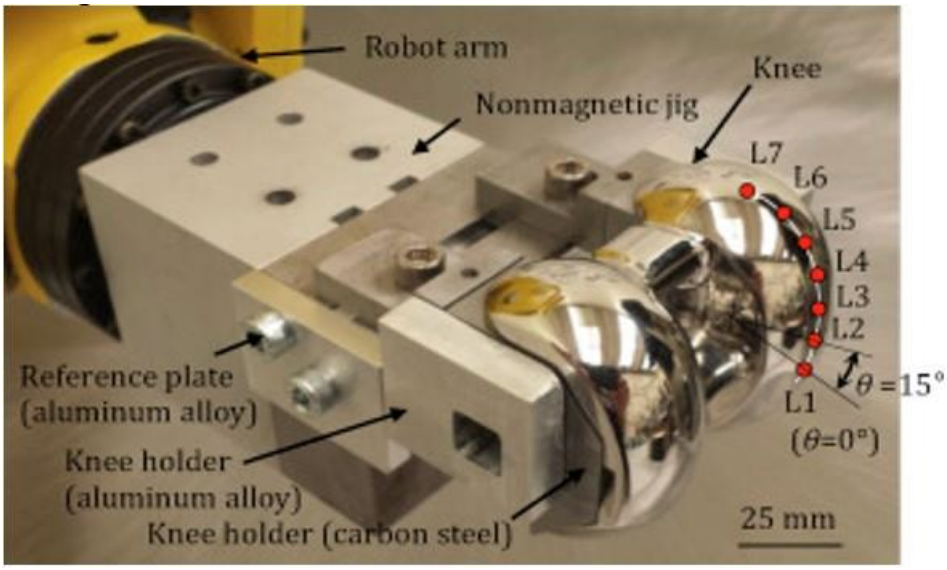

Figure 1.9: Tool holder designed to be compatible with the five-axis robot arm [40]

1.5 Research Gaps and Objectives

As stated earlier, there are many advantages in MAF including superfine finishing, better processing quality and controllability, a simple processing environment, and strong adaptability to the shape of the workpiece. The majority of applications for the MAF processes are focused on optical components and soft metal materials. However, there is a lack of research and exploration into the finishing possibilities of metallic materials with higher hardness in MAF applications. Furthermore, since MAF is a relatively new surface finishing technology, it is still considered an experimental approach for small workpieces rather than on large-area finishing for massive production in the manufacturing industry. Finally, while numerous statistical analyses focus on determining the optimal processing parameters for the MAF study, fewer studies delve into the investigation of MAF brush constituents, which form the fundamental basis of MAF's operational mechanisms. In addition, several studies implement the MAF process into freeform surface finishing such as for prosthetic parts, but a five-axis CNC machine or robot arm is necessarily required to achieve surface uniformity and consistency. However, the processing cost should be considered as well.

Therefore, the current study will fill gaps in understanding as follows:

1. Determine strategies for identifying optimal processing parameters using MAF on different metals such as mold steel, and a coated alloy sheet metal.

2. Develop a setup using MAF for a large area of the workpiece.

3. Explore the foundational principles that underly the constituents of MAF brushes, with a specific focus on the size of abrasive and iron particles.

CHAPTER 2: INVESTIGATION OF OPTIMAL PROCESSING PARAMETERS FOR DIFFERENT METALS BY MAF PROCESS

2.1 Introduction

Precise control of surface finish is critical for many engineering applications. This is especially true in tool and die production. As an example, an injection-molded part is directly related to the surface quality of a mold as any defect on the mold surface is directly transferred onto the surface of the final part [41]. Eliminating these defects is crucial for consumer products made by injection molding, requiring precise tolerances and a high-quality surface finish. Traditionally, a mold is machined from a large block to its near-net final shape using traditional machining processes such as milling, grinding, and nontraditional machining processes. The subsequent polishing process finishes the surfaces of the machined mold, which can consume a significant portion of mold production cost and time. According to Jones et al. [42], the time required for polishing can take up to 37% of total mold production time. More importantly, the polishing processes are carried out manually in a majority of industrial applications. Therefore, an automated process such as MAF may provide an alternative solution to manual polishing.

Even though there have been several studies on MAF on various materials, MAF on sheet metals has not been extensively studied. Sheet metals are one of the most widely used products in the automotive, aerospace, and household appliance industries due to their excellent strength-to-weight ratio [43]. For instance, for applications requiring both good formability and corrosion resistance, the interstitial-free steel sheet with a chromium (Cr) rich surface layer is a good solution to replace more expensive stainless steel 304 for applications needing corrosion resistance. The base metal forms a soft core, providing the formability needed in the sheet metal forming process due to its ductility, and the customized exterior layer provides protection from the corrosive environment. Previous studies indicated that it is very difficult to fine-polish such material (e.g.: OptiformTM, the trade name of a commercial grade produced by Arcanum Alloys Inc.) compared to, for example, the commonly used stainless steel 304. This is partially due to the presence of inert hard particles present on the surface layer in this proprietary process. Sheet metals modified with such compositions to yield desired properties can be manufactured using various manufacturing techniques like forming, drawing, etc. Surface finishing of chrome-coated sheet metals, or chromium alloyed surfaces, is especially important not only to retain certain desirable properties like corrosion resistance but also to improve durability and aesthetics.

Another important alloy class is titanium alloys. The most popular Ti-6Al-4V is widely used in the field of aerospace, medical industries, and additive manufacturing due to its outstanding corrosion resistance, good durability, low toxicity, high tensile strength, and high yield strength [44, 45]. However, titanium alloys are difficult to machine due to high chemical reactivity, low thermal conductivity, and low modulus of elasticity [46, 47]. The machined surface defects or compromised surface integrity lead to premature failure due to corrosion, wear, and fatigue, Therefore, enhancing and refining the surface quality becomes paramount in order to extend the service life. To achieve the required surface quality and to better control manufacturing quality, a few researchers recently used MAF to finish titanium alloys [48, 49].

2.2 Objectives

The primary objective of this section is to investigate whether the MAF process can be applied to different metals and find the optimal processing parameters via statistical analysis such as the design of experimental method and fractional factorial design. Statistical analysis enables to efficiently investigate and analyze the effects of multiple factors on a process or system, specifically by examining various parameters for their main and interaction effects on achieving surface finishing for HP4M mold steel and AISI S7 steel and by obtaining the optimal MAF brush composition and conditions for chrome-coated low-carbon steel sheet, respectively.

2.3 MAF on HP4M Mold Steel

2.3.1 Experimental Setup

MAF was performed on the pre-ground mold steel (HP4M, Hitachi Metals; Santa Clara, CA) using a custom-made tool as shown in Figure 2.1. Three Neodymium ring (permanent) magnets (5mm x 32mm) were connected to the magnet holder, which was made of aluminum to prevent unintended attraction of the brush constituents. This holder was mounted onto the spindle of HAAS VF4 CNC milling which controls the rotational speeds, surface feed rate, and tool gap distance.

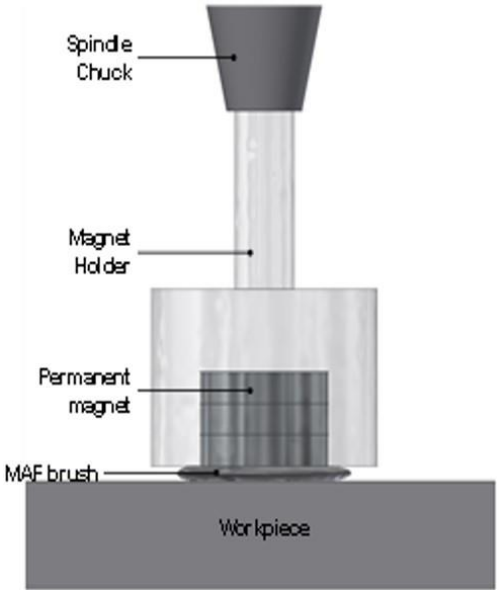

Figure 2.1: Schematic of the magnetic tool holder

2.3.2 Preparation of MAF Brush

The brush was made of black ceramic (BC) particles (mostly Silicon Carbide) provided by Beta Diamond Products (Yorba Linda, CA) and iron particles (with an average size of 150 µm, Carolina Biological Supply Company; Burlington, NC) mixed with silicone oil (1,000,000 CGS, ShinEtsu; Akron, OH) in a 1:1:1.5 ratio, by weight. Exfoliated graphite nanoplatelets (xGnP, XG science; Lansing, Mi) were added to the brush, which functions as a nano-scale solid lubricant. Based on the work, the addition of xGnPs significantly extended the brush life and improved the final surface quality [19, 50].

2.3.3 Workpiece and Roughness Measurement

Pre-ground mold steel (HP4M) blocks with dimensions of 60 x 60 x 20 mm were used as the workpiece. The name of the HP4M is derived from LG company and is specifically designated. The chemical composition of this particular steel type is detailed in Table 2.1. The surface condition was characterized by using a surface profilometer (Zeiss Surfcom Touch). Multiple measurements were taken in the perpendicular direction to the original grinding marks of the workpiece. The average surface roughness (Ra) was found to be 360 nm. In order to enhance the polishing efficiency, all the tool paths were set to be perpendicular to the original grinding marks, as shown in Figure 2.2. For each path, the tool traveled the entire length of the workpiece (60 mm) with a constant rate of 3.1 inches/min. The MAF processing time for each experiment was 2.5 hours.

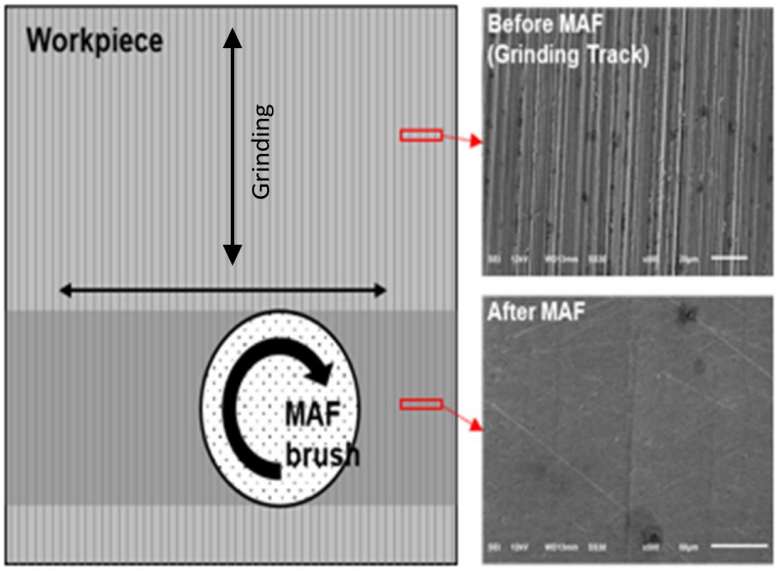

Figure 2.2: Designed tool path of MAF (left). The tool path is perpendicular to the grinding direction. Surface patterns before (upper right) and after (lower right) MAF process

Table 2.1: Chemical composition of HP4M mold steel

	C	Si	Mn	Cr	Mo	Fe
HP4M	0.32-0.38	0.2-0.4	0.6-1.4	1.6-2.0	0.4-0.6	Added

2.3.4 Methodology

A 2^{k-1} fractional factorial design (FFD) was adopted to evaluate the impact of processing parameters. It is a type of experimental design used in statistics and experimental research to efficiently investigate the effects of a set of factors on a response variable. The 2^{k-1} refers to the number of factors and their levels included in the design. Specifically, the "k" represents the number of factors, resulting in a total of 2^k combinations. However, the "k-1" indicates that a subset of these combinations will be used in the fractional factorial design to reduce the total number of experimental runs. In this study, the processing parameters are wt. % of xGnPs, spindle speed, BC size, and gap distance, with the evaluated response of final surface quality in terms of surface roughness. Following the statistical method, high and low levels were selected for each processing parameter as listed in Table 2.2. A full 2^k Factorial Design calls for a total of 16 experiments while the number of experiments was reduced to 2^3 (=8) using the FFD analysis. The purpose of using

FFD design was to economically investigate cause-and-effect relationships of significance in each experimental setting.

Table 2.2: Experimental levels for selected MAF parameters on HP4M mold steel

Level	xGnPs (wt. %) (1)	Spindle Speed (RPM) (2)	BC Size (μm) (3)	Gap Distance (mm) (4=123)
Lower (-)	0.2	400	18	1
Higher (+)	0.8	1600	940	3.0

The level settings for each of the eight experiments can be found in Table 2.3 where the "+" and "-" symbols represent the upper and lower levels whose values are listed in Table 2.2. The four processing parameters, wt. % of xGnPs, spindle speed, BC size, and gap distance, are denoted as labels 1 to 4, respectively. The interaction between two parameters can be represented by the combination of labels 1 to 3, which is also confounded with any interaction with gap distance. For example, the interaction between xGnP and spindle speed is represented by label 12. After each MAF test, the surface characteristics were quantified by the average surface roughness, Ra, measured at five different locations using the surface profilometer, which can be found in the last column in Table 2.3.

Table 2.3: Design matrix by using 2^{4-1} fractional factorial method on HP4M mold steel

Test	1	2	3	12	13	23	4=123	Ra (nm)
1	-	-	-	+	+	+	-	333
2	+	-	-	-	-	+	+	356
3	-	+	-	-	+	-	+	223
4	+	+	-	+	-	-	-	193
5	-	-	+	+	-	-	+	354
6	+	-	+	-	+	-	-	289
7	-	+	+	-	-	+	-	325
8	+	+	+	+	+	+	+	354

2.3.5 Experimental Result and Discussion

Once the final roughness had been measured, the effectiveness coefficients (E) for each processing parameter were established following the FFD model. These results are shown in Table 2.4, where the effectiveness coefficient on surface roughness was determined by averaging the difference of the final roughness values obtained at higher and lower levels of each processing parameter.

Table 2.4 Effectiveness coefficient for each parameter on HP4M mold steel

	xGnPs (wt. %)	Spindle Speed (RPM)	BC Size (μm)	Gap Distance (mm)
Effectiveness Value	-11.29	-58.62	54.10	37.77

Considering the magnitude of the values in Table 2.4, the significance of spindle speed and BC size in determining the final surface quality is evident as they exert the greatest influence. Conversely, the impact of gap distance is comparatively low while the wt.% of xGnPs has the least effect on the final surface finish quality. Consequently, the final surface finish quality of the workpiece can be improved further by increasing spindle speed and the wt. % of xGnPs while decreasing BC size and gap distance. These results were expected based on previous knowledge from the grinding process, which functions similarly to the MAF process.

To visualize the interdependency among the processing parameters, two-way diagrams were generated. Figures 2.3 to 2.5 represent the interdependencies between wt. % of xGnPs and spindle speed, spindle speed, and gap distance, and spindle speed and BC size, respectively. Figure 2.3 shows two lines representing 400 and 1600 RPMs as a function of the wt. % of xGnPs are pretty much in parallel despite the minute differences. From this result, it can be concluded that wt. % of xGnPs has an insignificant interdependence with spindle speed. The two nearly parallel lines presented in Figure 2.4 indicates that the interdependence between the spindle speed and the gap distance is negligible. The occurrence of parallel lines arises from the reduction in roughness value that happens to a similar extent when increasing the spindle speed in both levels of gap distance, namely 1mm and 3mm, respectively.

However, as the spindle speed increased from 400 RPM to 1600 RPM, the utilization of different grit sizes of BC resulted in varying changes in the average Ra value. When the 18 μm BC was employed, the average Ra value exhibited a decrease from 344 nm to 208 nm. Conversely, when

the 940 µm BC was utilized, the average Ra value experienced an increase from 320 nm to 340 nm as shown in Figure 2.5. This suggests a notable interconnectedness between the two processing parameters. In simpler terms, altering one parameter necessitates the consideration of the other as they mutually influence each other. It also implies that it is better to use higher spindle speeds for smaller BC sizes but slower spindle speeds for larger BC sizes.

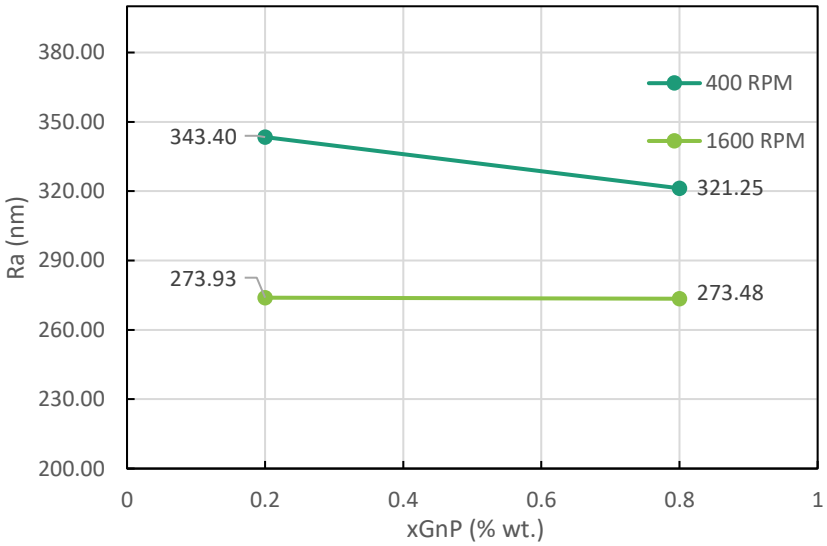

Figure 2.3: Two-way diagram between weight fraction of xGnPs and spindle speed shows the insignificant interdependence between these two parameters

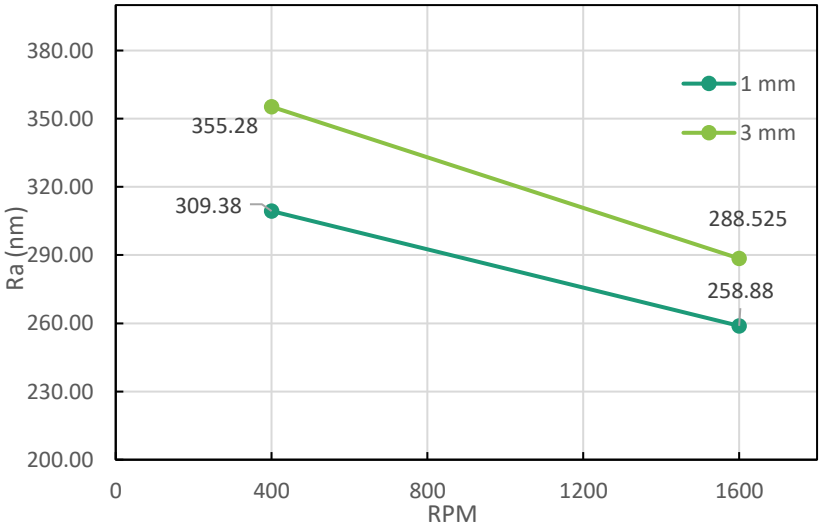

Figure 2.4: Two-way diagram between spindle speed and gap distance shows the small interdependence between these two parameters

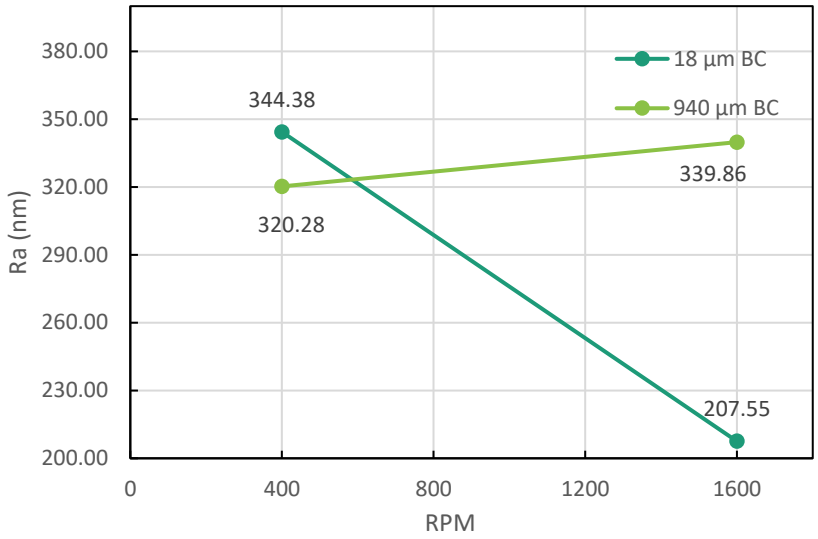

Figure 2.5: Two-way diagram between spindle speed and BC size shows the significance of independence between these two parameters

Based on these results, an additional experiment was performed to find the optimal parameters for the first step of a multi-step progressive MAF process. Since the main and interdependence effects of spindle speed, BC size, and gap distance had the largest impact on the final Ra, additional levels of spindle speed and gap distance were added with the intermediate sized of BC (125 µm) to carry out the optimal processing parameters of spindle speed and gap distance. To expand the scope of this experiment, an additional spindle speed of 1200 RPM and a gap distance of 2mm were introduced. Consequently, the experimental setup now includes spindle speeds of 800, 1200, and 1600 RPM, along with gap distances of 1, 2, and 3 mm. A BC size of 125 µm was selected based on the initial surface roughness because the larger abrasive particles should be used on the rougher initial surface by quickly removing the majority of surface defects. To achieve a higher-quality surface finish, it is necessary to employ finer abrasive particles in the subsequent steps. The content of xGnPs was fixed at 0.3 wt. % as it was found to be the least significant factor as shown in Figure 2.3.

Figure 2.6, which has the results of this supplemental experiment, illustrates the relationship between the Ra value and RPM for three distinct gap distances. As the spindle speed increased, the Ra value also increased for each gap distance. At 800 RPM, the Ra value decreased as the gap distance decreased as expected. However, this pattern did not persist for the Ra values at 1200 and 1600 RPM. This deviation can be attributed to the expulsion of certain brush constituents due to

the high centrifugal forces experienced at high spindle speeds of 1200 and 1600 RPM, combined with a 1 mm gap distance, as shown in Figure 2.7. Notably, the loss of brush constituents, particularly the abrasives, significantly impairs the performance of MAF, which was not observed at lower spindle speeds.

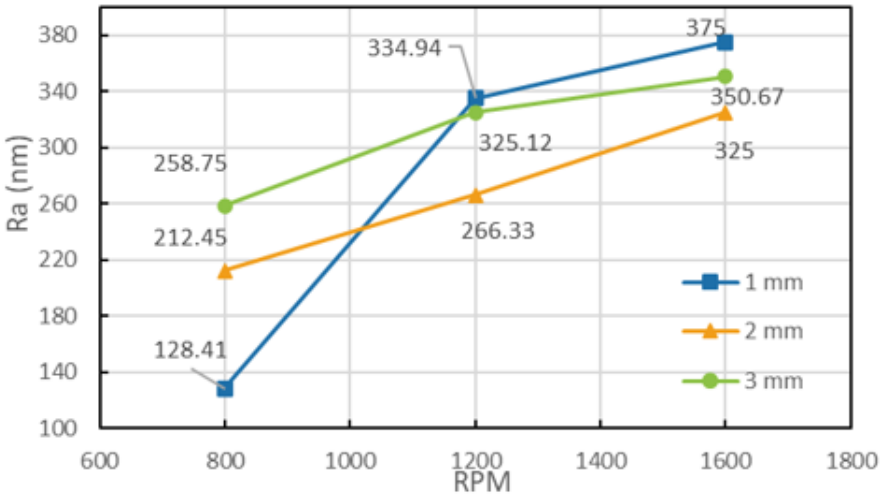

Figure 2.6: Surface roughness (nm) versus spindle speed for different distance levels with 125 µm BC size

Figure 2.7: The comparison of MAF brush before (left) and after MAF (right). The expulsion of brush constitutes is at a higher spindle speed and lower gap distance

In implementing the MAF for any practical application such as mold surface finish, a multi-step MAF process was designed. Based on the results from this study, each MAF step was to finish an entire flat workpiece surface gradually as shown in Table 2.5. Step 0 represents the initial surface with Ra of 434 nm. Throughout the steps, the BC size was progressively refined from 125 µm to

3 µm, as the larger abrasive particles increased the material removal rate while the smaller abrasive particles were required to achieve a smoother surface. Spindle speed and gap distance were also adjusted between steps as it was found that both factors had significant interdependency with BC size. The surface finish attained in each step is presented in Figure 2.8. The final Ra value achieved was measured to be 26 nm, which is comparable to the Ra of 20 nm achieved using manual polishing (Diamond 3000 grit). To compare the results of MAF to manual polishing, Figure 2.9 shows the two samples by MAF and manual polishing side by side, reflecting the text printed on a sheet of paper.

Table 2.5: Progressive MAF setting and final surface roughness for HP4M mold steel

Step	xGnP (wt.%)	Spindle Speed (RPM)	BC Size (μm)	Gap Distance (mm)	Ra (nm)
0	-	-	-	-	434
1	0.3	800	125	1	194
2	0.3	1200	40	2	168
3	0.3	1200	18	2	42
4	0.3	1200	3	2	26

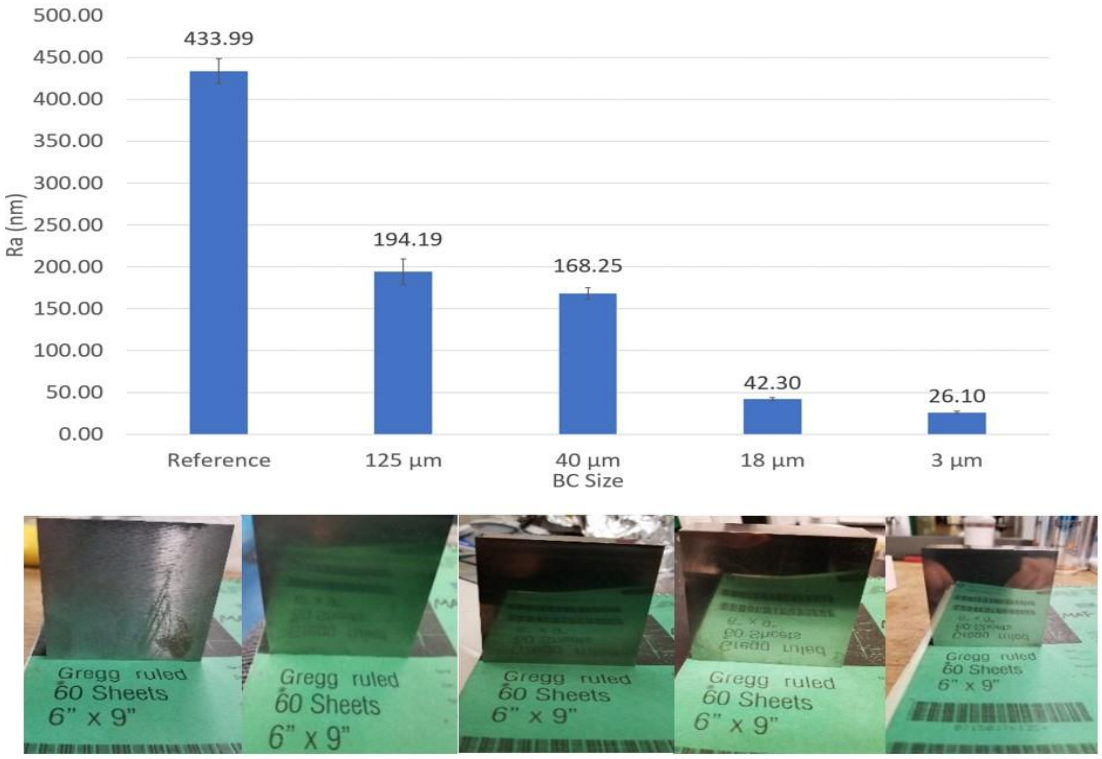

Figure 2.8: Surface roughness value after stepwise MAF process

Figure 2.9: Surface finish comparison between progressive MAF polishing (Ra 26nm) (left) and manual polishing (diamond 3000 grit, Ra 20 nm) (right)

2.3.6 Conclusion

This study presents a 2^{k-1} FFD (Fractional Factorial Design) aimed at optimizing several key processing parameters, namely wt.% of xGnP, spindle speed, abrasive size, and gap distance. The main objective is to enhance the surface roughness of HP4M mold steel by using the MAF process. It is important to note that, despite numerous parameters yet to be optimized, this study primarily focuses on the aforementioned variables. Based on analysis of the results, it was concluded that: spindle speed was found to be the dominant factor over the final Ra as it had the largest effectiveness coefficient, followed by BC size, gap distance, and wt. % of xGnP with the effectiveness coefficients of -58.62, 54.10, 37.77, and -11.29, respectively. Spindle speed and BC size were the only factors found to have significant interdependency. Leveraging the knowledge from the FFD, a multi-step MAF process was designed that a slower spindle of 800 RPM and a lower gap distance of 1mm should be applied with larger BC particles rapidly removing surface irregularities. Subsequently, a higher spindle speed of 1200 RPM and a larger gap distance of 2 mm should be adopted for finer finishing. The final Ra value of 26 nm was achieved by this multi-step MAF process which is comparable to that of the manual polished sample with Ra of 20 nm.

2.4 MAF on Chrome (Chromium alloy)-Coated Sheet Metal

The primary objective of this study is to apply MAF on the surface of chromium alloyed low-carbon sheet metal samples provided by Arcanum Alloys (our collaborator) and to understand the effect of various processing parameters reaching the final surface quality of the workpiece.

2.4.1 Experimental Setup

The conducted experimental setup for chrome-coated sheet metal surface finishing was the same as the MAF process on HP4M mold steel which is in section 2.3.1.

2.4.2 Preparation of MAF Brush

The brush was made of various-sized black ceramic (BC) particles (Beta Diamond Products; Yorba Linda, CA), cubic boron nitride (cBN) abrasives (LANDs super abrasives; New York, NY) or mass media alumina abrasives (Rosler Metal Finishing USA, LLC; Battle Creek, MI), and iron particles (with an average size of 150 μm, Carolina Biological Supply Company; Burlington, NC) mixed with silicone oil (DM-1,000,000 CGS, ShinEtsu; Akron, OH).

2.4.3 Workpiece Material

The workpiece used in the experiment was the chromium-alloyed low-carbon steel sheet provided by Arcanum Alloys (Kentwood, MI). The substrate metal was made of interstitial-free (IF) steel, low carbon steel, cold rolled to a thickness of 1 mm foil from a thick slab. Later, a proprietary slurry that contains chromium (Cr), was applied continuously to the surface of the sheet substrate. Then, the slurry-coated coil was annealed in a controlled atmosphere at high temperatures, during which the Cr particles migrate and diffuse into the base metal substrate. At the same time, Fe atoms diffuse to fill in the interstitial space among Cr particles and, consequently, Cr-rich layers are metallurgically formed at both sides of the sheet metal. Figure 2.10 shows the energy dispersed spectroscopy (EDX) elemental mapping across the sample thickness, which clearly shows the 50 μm thick Cr-rich (nearly 20 wt. %) surface layers.

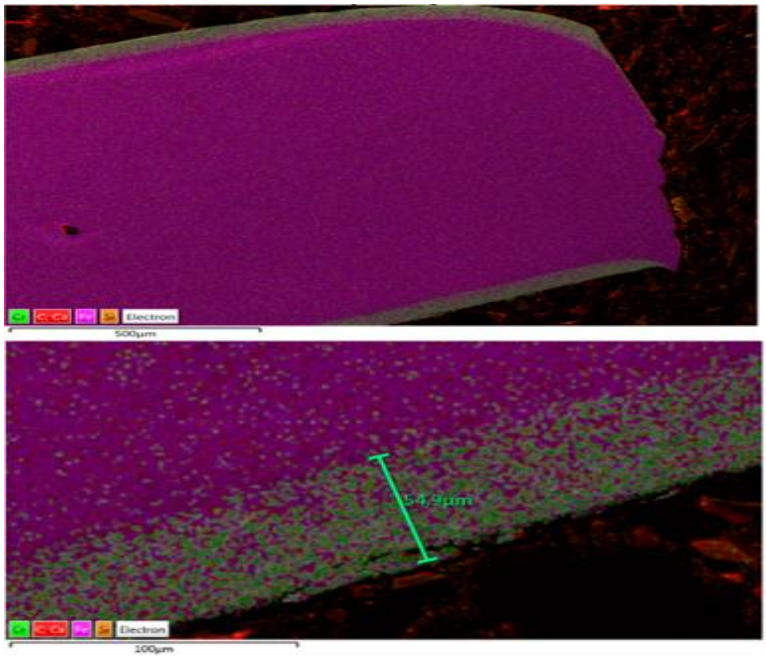

Figure 2.10: SEM image of the chrome-coated low-carbon steel sheet metal. The main dark pink color depicts the low-carbon steel substrate and the green layer is the thickness of the chromium

2.4.4 Methodology

As chrome-coated sheet metal polishing has not been widely studied with MAF, the identification of suitable processing conditions is the crucial step in achieving the final goal of achieving nano-scale surface roughness. Hence, different abrasives like cBN, BC, and alumina, and various sizes of abrasives were explored in this study. Similarly, brush composition plays a vital role in the material removal process in the MAF. The overall stiffness of the brush changes the indentation depth of the abrasives and thus dictates the material removal from the surface of the workpiece. Depending on the initial roughness and hardness of the workpiece, the brush composition also needs to be determined properly either by reducing the silicone oil to increase the stiffness of the MAF brush or adding the content of iron particles to increase the magnetic strength of the MAF brush. Hence, various weight composition of the brush and their impact on the final surface roughness of the substrate material were studied. Finally, the finishing time was optimized to increase the efficiency of the MAF process.

2.4.5 Experimental Result and Discussion

Selecting an appropriate type of abrasive for a given material is an important factor associated with the MAF process as the hardness, durability, and cost of the abrasives vary. In the initial experiment, three types of abrasives (alumina, cBN, and BC) were introduced. The size of each

abrasive was around 300 µm. After MAF was applied with the spindle speed of 600 RPM on each sheet metal sample for 5 hours, it can be observed that all three types of abrasives decreased the final surface roughness as shown in Figure 2.11. BC is the most effective, followed by cBN and alumina which is the least effective among all. The surface roughness value after MAF with BC decreased to 738 nm whereas the surface roughness of the samples after MAF with alumina and cBN were 1003 and 852 nm, respectively. Thus, BC was chosen for further experiments in this study. The final surface roughness attained through MAF with alumina was higher than the other two abrasives possibly because the hardness of alumina is the lowest among all the abrasives. This may have reduced the abrasion for alumina abrasives, reducing the material removal rate. Even though the hardness of cBN is higher than BC, the surface finishing of using cBN particles was not as good as using BC particles. This is due to the cutting edges of the BC particles being shaper than the cBN particles, as shown in Figure 2.12. Given the presence of those sharp edges, the BC particles are more efficient in abrading the workpiece. Consequently, based on the experimental results, the use of BC particles is necessary to improve the effectiveness of the MAF for surface finish.

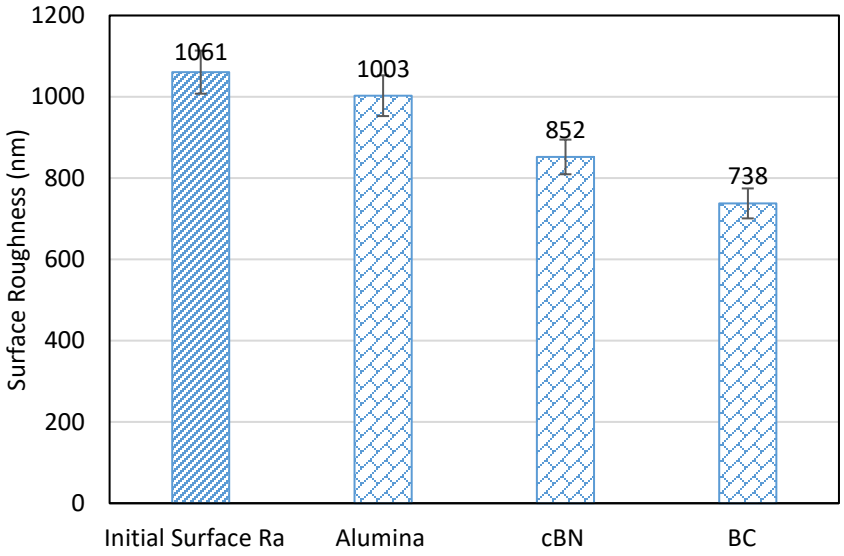

Figure 2.11: Surface roughness variation with different types of abrasives

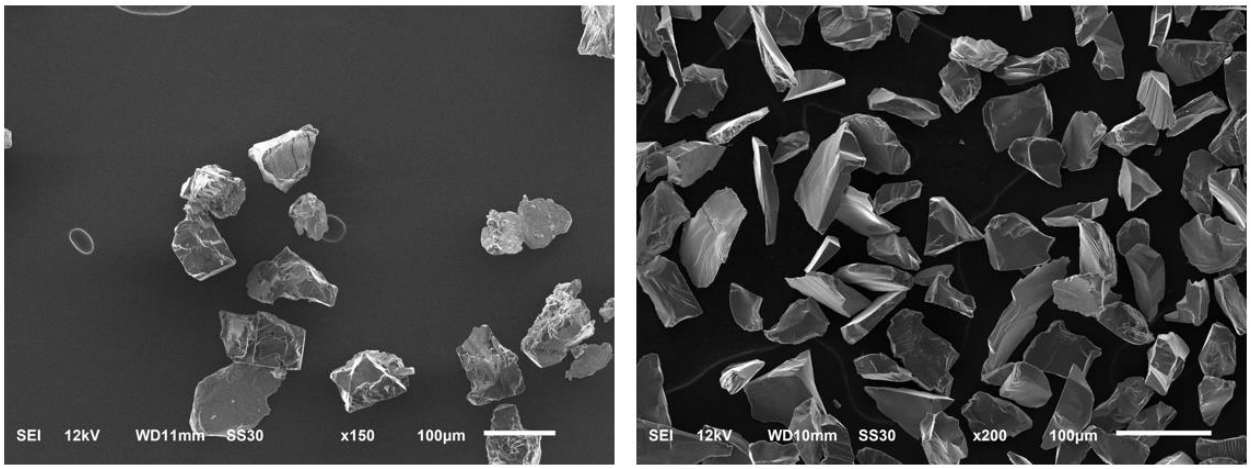

Figure 2.12: SEM of cutting edge for cBN (Left) and BC (Right) particles

Not only the types of abrasives but also the size of abrasives are important factors in affecting MAF performance. Another experiment was conducted to determine the effect of abrasive size in the MAF process. The size range of the BC abrasives varied from 940 to 3 µm with five distinct sizes of BC, as shown in Figure 2.13. The findings demonstrated the consistent trend of diminishing surface roughness values with decreasing abrasive size. The phenomenon mentioned can be explained by considering that in the MAF process with the constant total mass of the abrasives, the use of smaller abrasive particles results in better engagement and an enhanced surface finishing process. One anomaly was observed with the 940 µm sized BC, which yielded a surface roughness of 1931 nm after MAF as shown in Figure 2.13. The final roughness value exceeded the initial surface roughness. Upon inspection of the surface, there were rotational scratching and pitting marks on the surface. This was due to the large abrasive particles significantly scratching the surface which would result in severe scratching and pitting marks, deteriorating the surface quality.

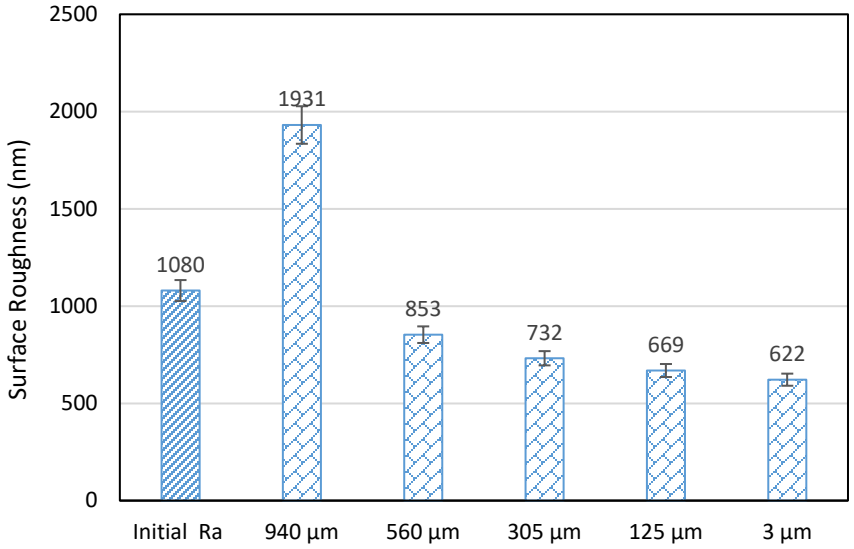

Figure 2.13: Surface roughness variation with different sizes of black ceramic abrasives

The composition of the MAF brush is one of the most crucial factors affecting the MAF process. To understand the impact of the content of liquid media, the following experiments were conducted with different weight fractions of silicone oil in the MAF brush. All the previous experiments used the brush composition of 1:1:1.5 by weight ratio in terms of iron particles, abrasives, and silicone oil. The weight ratio of the silicone oil was reduced as shown in Figure 2.14. The reduction in the weight ratio of the silicone oil in the MAF brush improved the efficiency of the surface finishing process. The surface roughness was reduced nearly by half of the initial roughness with the 305 and 125 µm abrasives. Furthermore, the surface roughness dropped even more substantially (down to 92 nm) with the 3 µm sized BC. The outcome is valid since using a smaller proportion of silicone leads to a firmer and stiffer MAF brush. Thus, it would provide a higher normal force to the workpiece in comparison to a higher fraction of silicone in the MAF brush. Consequently, this will increase the material removal rate and improve surface roughness.

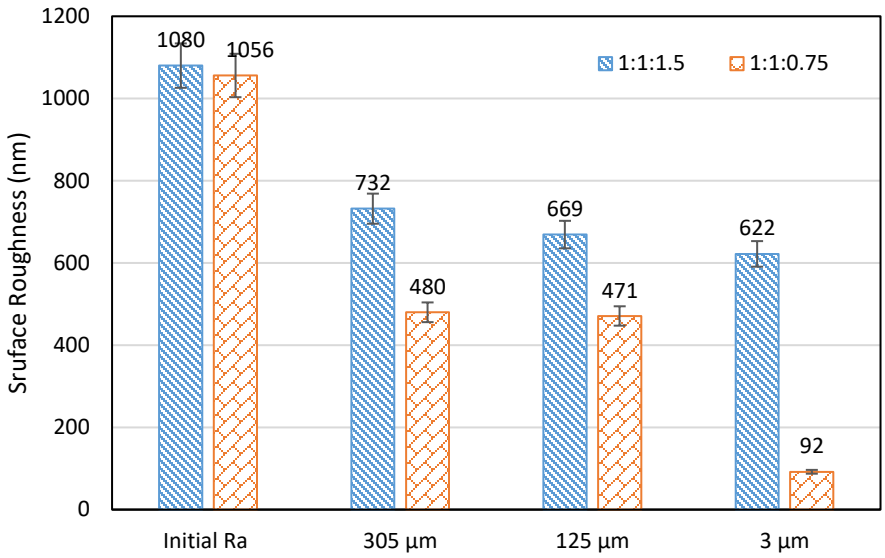

Figure 2.14: Surface roughness variation with two different compositions of MAF brush in different sizes of BC

Later, a stiffer MAF brush was introduced by adding a higher weight fraction of iron particles. The weight fraction was changed to 4:1:1.5 in terms of iron particles, abrasives, and silicone oil, which improved the yield stress and stiffness of the brush. This resulted in a better surface finish, as shown in Figure 2.15. The weight fraction of 4:1:1.5 in the experiment proved to be the most effective among all the combinations due to the increase in magnetic strength by adding more weight fraction of iron particles. However, the brush composition of 4:1:0.75 was too stiff because of the lacking of silicone oil, yet making excessive indentations [51] on the workpiece. The final surface roughness of 38 nm was achieved with the MAF brush whose weight fraction was 4:1:1.5. It can be explained by the fact that the chain structures grew in a dense column of higher concentrations of iron particles in the MAF brush. This will result in higher material removal from the surface of the workpiece and can help achieve better final surface roughness.

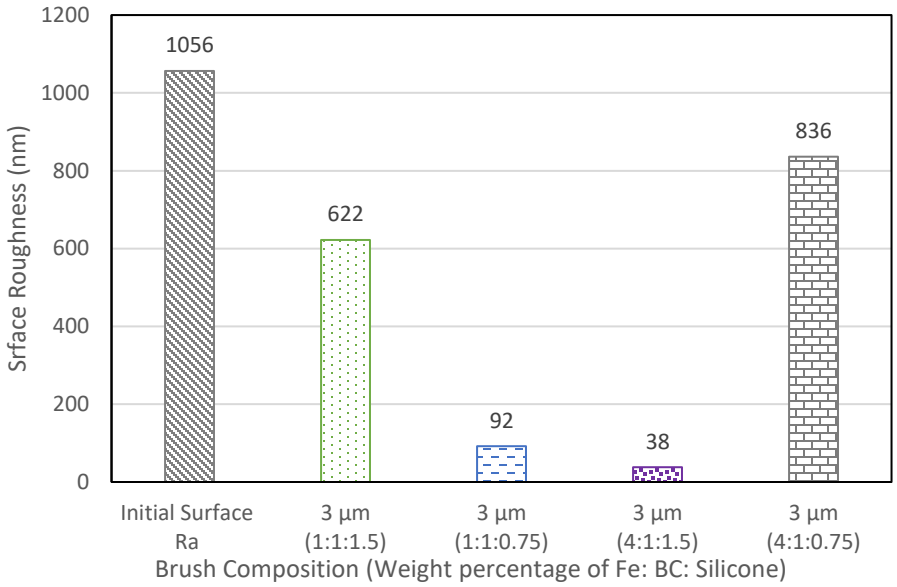

Figure 2.15: Surface roughness variation with three different compositions of MAF brush with 3 µm black ceramic

The processing time is directly related to processing efficiency. Workpiece samples were polished using the 4:1:1.5 weight ratio of iron particles, 3 µm black ceramic, and silicone oil and the surface roughness was measured at three distinct times. After each time period, samples were cleaned before measuring the surface roughness. The surface roughness of the sample after 1.25 hours, 2.5 hours, and 5 hours are shown in Figure 2.16. It shows that the surface roughness exhibited an exponential decrease during the initial hour of the MAF process. However, it reached a point of saturation after a certain time. Specifically, the roughness value was stabilized to 47.33 nm after approximately 2 to 2.5 hours. Consequently, the processing time of 2.5 hours is chosen to be the optimal duration for the sheet metal.

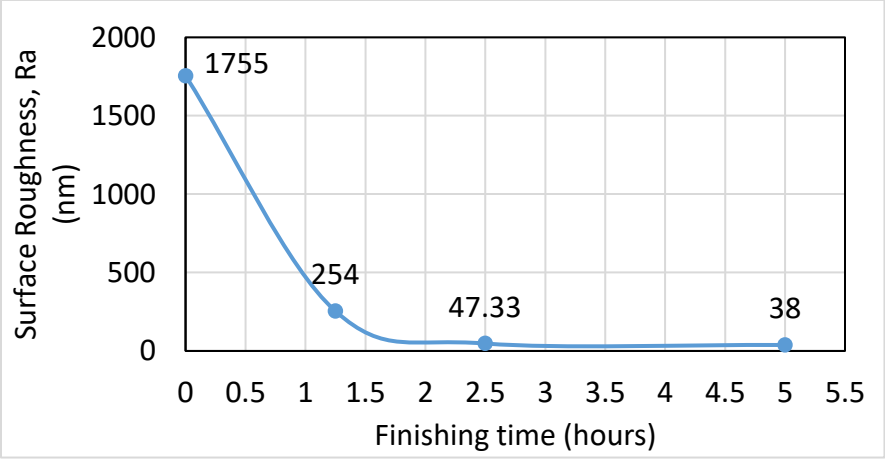

Figure 2.16: Surface roughness variation with time

2.4.6 Conclusion

The optimum processing parameters were investigated for polishing chrome-coated sheet metal samples using the MAF process. The final average surface roughness, Ra, as low as 38 nm, was obtained from the initial roughness of 1755 nm via the MAF process with the design of the experiment. Among all the different types of abrasive, BC performed the best surface finishing result, followed by cBN and alumina. Moreover, the smallest size of BC (3 μm) yielded the best surface finish. This was attributed to the increased engagement of abrasive particles throughout the MAF process. Significantly, it was discovered that employing a stiffer brush containing a greater proportion of ferromagnetic particles by weight proves to be more efficacious in the MAF performance on sheet metal samples. The reason behind this phenomenon can be attributed to elevated magnetic field strength, resulting in a greater normal force exerted by an individual abrasive due to the increased content of iron particles present in the brush. However, the inadequate amount of silicone oil leads to an undesired stiffening of the brush. Additionally, the high yield stress of the brush causes excessive indentation on the workpiece, ultimately deteriorating its surface finish.

2.5 MAF on AISI S7 Mold Steel

The primary objective of this study is to optimize the processing parameters for finishing AISI S7 mold steel metal with the MAF process. Similar procedures and methodology were used to find the optimal processing parameters on HP4M mold steel. In this section, the parameter of wt. % of xGnPs was replaced by the weight ratio of MAF brush composition because the former was found to be the least effective parameter in section 2.3 but the weight ratio of MAF brush composition had a significant influence on MAF finishing performance which could be found in section 2.4. Additionally, the feed rate of the abrasive tool instead of the abrasive size was chosen to be studied to see how much impact this parameter has in the MAF process.

2.5.1 Experimental Setup

In this study, the experimental setup was the same as the MAF process on HP4M mold steel as shown in section 2.3.1. However, The transition was made from using ring magnets to employing a single ball magnet measuring 0.5 inches in diameter to accommodate the forthcoming investigation into finishing intricate geometries with freeform surfaces, as shown in Figure 2.17. The MAF processing time would be 30 or 15 minutes depending on the feed rate.

Figure 2.17: The 0.5-diameter ball magnet with its machined holder

2.5.2 Preparation of MAF Brush

The brush was made of BC particles (3 μm) and iron particles (with an average size of 150 μm) mixed with silicone oil (1,000,000 CGS) in 1:1:1.5 and 4:1:1.5 weight fractions.

2.5.3 Workpiece and Roughness Measurement

The pre-ground AISI S7 mold steel workpieces with dimensions of 35 x 35 x 10 mm were used. AISI S7 steel is a shock-resistant air-hardening steel. It has exceptional impact properties with the highest hardenability of shock-resisting mold steel grades. AISI steel S7 also possesses hot work capabilities. Since S7 steel is hardenable in the air, it is safe and stable in the air environment. The stylus profilometer was used again to measure the surface roughness of the workpiece. As the initial surface roughness was varied from pre-ground techniques, the percentage of change in roughness value before and after the MAF process will be treated as the credential (effectiveness coefficient).

2.5.4 Methodology

A 2^{k-1} fractional factorial design (FFD) was adopted to evaluate the impact of the four main processing parameters (k=4) on the final surface quality, which include spindle speed, the weight ratio of MAF brush composition, the gap distance between the workpiece and magnet, and the feed rate of the brush. Using this statistical method, higher and lower levels were selected for each processing parameter as listed in Table 2.6.

Table 2.6: Experimental levels for selected MAF parameters on AISI S7 steel

Level	Spindle Speed (RPM) (1)	Brush Composition (wt. ratio) (2)	Gap Distance (mm) (3)	Feed Rate (in/min) (4=123)
Higher (+)	2000	4:1:1.5	2	6.2
Lower (-)	800	1:1:1.5	1	3.1

The level settings for each of the eight experiments can be found in Table 2.7 where the "+" and "-" symbols represent the upper and lower levels whose values are listed in Table 2.6. The four processing parameters, which are spindle speed, weight ratio of MAF brush composition, gap distance, and feed rate are denoted as labels 1 to 4, respectively. The percentage change in average roughness value was recorded in Table 2.7.

Table 2.7: Design matrix by using 2^{4-1} fractional factorial method on AISI S7 steel

Test	1	2	3	4=123	Response % ΔRa
1	+	+	+	+	88.11
2	-	+	+	-	88.20
3	+	-	+	-	79.61
4	-	-	+	+	11.14
5	+	+	-	-	89.70
6	-	+	-	+	66.54
7	+	-	-	+	69.23
8	-	-	-	-	47.88

2.5.5 Experimental Result and Discussion

In this study, Minitab statistical analytic software was used to determine the main and interaction effects over the four processing parameters, spindle speed, weight ratio of MAF brush composition, gap distance, and feed rate. Considering the slope of each line segment in Figure 2.18, the magnitude of the slope demonstrates that MAF brush composition had the largest impact, followed by spindle speed, feed rate, and gap distance, in terms of percent change in surface roughness value.

Figure 2.18 shows that the higher rotational speed of the spindle and weight ratio of MAF brush composition will lead to a higher percentage of change in roughness, whereas gap distance and feed rate will bring a lower percent change in surface roughness. This is indicated by the sign of the slope (increasing or decreasing).

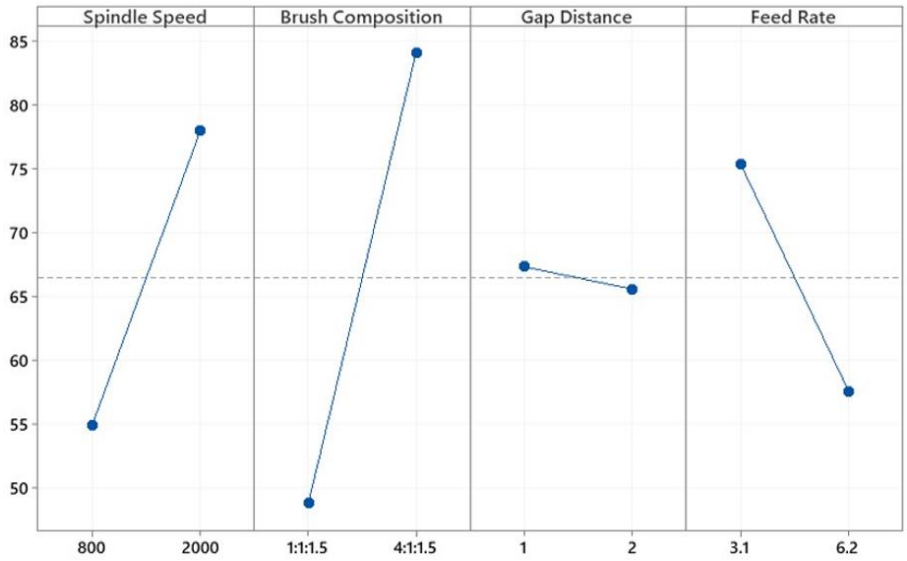

Figure 2.18: The main effect of each parameter on the percentage of change in surface roughness

The interaction effect between spindle speed and brush composition is the most significant which means that changing one parameter intimately impacts the other, as shown in Figure 2.19. The best way to change surface roughness was to use the processing parameters with higher spindle speed and higher brush composition. A higher concentration of iron particles in the MAF brush leads to increased stiffness and magnetic force when exposed to a magnetic field. Consequently, the material removal rate improves, resulting in a higher percentage of surface roughness alteration. Using a faster spindle speed not only enhances the dynamic motion of abrasives but also leads to a greater reduction in surface roughness compared to employing a slower spindle speed. Figure 2.19 illustrates the relationship between various factors, including gap distance and spindle speed, feed rate and spindle speed, brush composition, and gap distance, and brush composition and feed rate. The findings reveal a limited interdependence among these factors. It was also observed that larger gap distances were favored by a higher brush composition and higher spindle speed because a higher weight fraction of iron particles would possess higher magnetic strength within the MAF brush. This higher strength, in turn, contributed to the structural integrity of the iron particle column formations, preventing their breakdown even when a larger gap distance was employed. In addition, a higher weight fraction of iron particles, though leading to a more rigid MAF brush,

could be extruded more from the entire brush when a smaller working gap distance was employed. The excessive loss of brush constituents could adversely impact finishing efficiency. On the contrary, a smaller working gap distance was linked to lower brush composition and spindle speed. In this context, the lower brush composition was capable of sufficiently occupying the gap, while the reduced presence of iron particles prevented them from being expelled due to centrifugal force with a lower spindle speed. Additionally, it was consistently observed that slower feed rates resulted in a higher percentage change in roughness value across all scenarios.

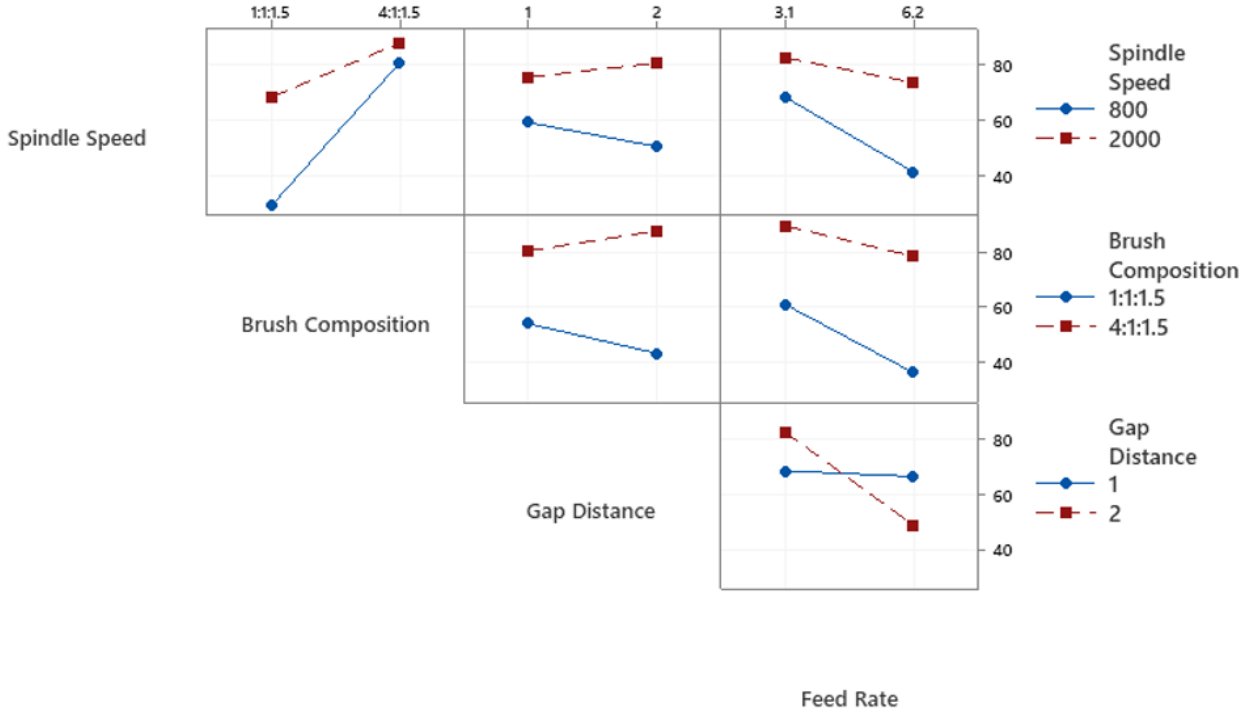

Figure 2.19: The interdependence between different two parameters in the percentage of change in surface roughness

Based on the interaction plot, the optimal processing parameters were identified. These parameters included a higher spindle speed with 2000 RPM, and a higher concentration of iron particles in the MAF brush, with a weight fraction of 4:1:1.5 for iron, BC, and silicone oil, respectively. The working gap distance was set at 2 mm and a slower feed rate of 3.1 inches/minute was employed. As a consequence of these optimized settings, the final roughness value improved significantly, decreasing from 507 nm to 45 nm. Moreover, the reflective text on the sample working path after the MAF process was visible, as depicted in the leftmost vertical path in Figure 2.20. The other two paths were classified as MAF finishing the surface in different surface inclined angles, to study MAF on simplified freeform geometry. As this study primarily focused on the MAF performance

of the horizontally flat sample, further investigation into the two tentative experimental paths will be conducted in future research.

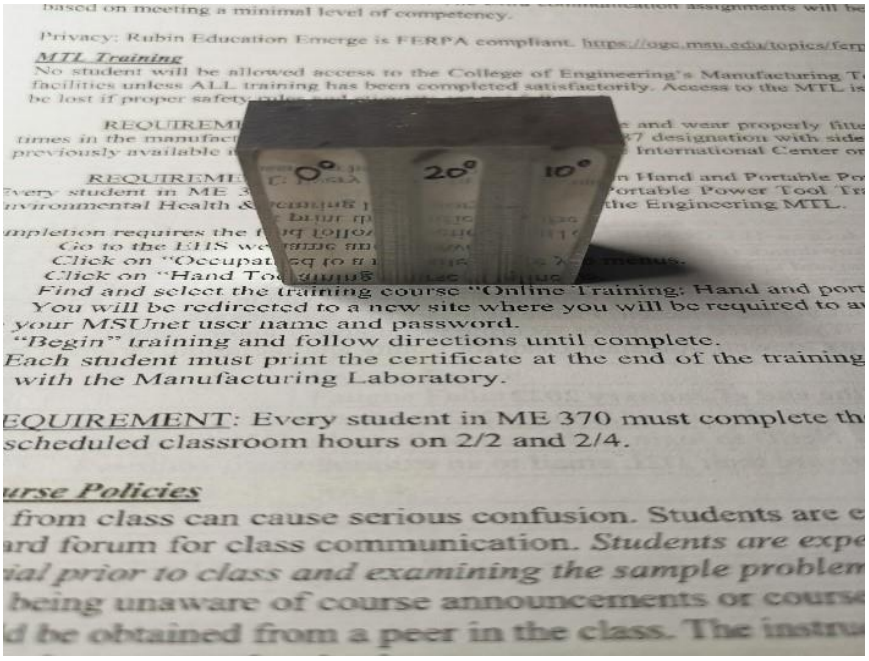

Figure 2.20: The surface finish of AISI S7 steel after applying optimal processing parameters on a flat sample (leftmost path)

2.5.6 Conclusion

In this study, a 2^{k-1} FFD was introduced to optimize processing parameters including spindle speed, the weight ratio of MAF brush, gap distance, and feed rate of the abrasive tool. The weight ratio of the MAF brush was the most dominant factor followed by spindle speed, feed rate, and gap distance. There was a significant interdependence between the weight ratio of MAF brush composition and spindle speed. A higher weight ratio of iron particles in the brush composition and higher spindle speed with a lower feed rate and larger gap distance provided a better percentage change in surface roughness.

2.6 Proposed Future Work

Future work will be conducted to address the different aspects of the existing analytical results and the improvement of the experimental setup.

1. Many other abrasive sizes will be included in the design of experiment (DOE) analysis as only two sizes of abrasive (3 μm and 940 μm) were investigated in a fractional factorial design (FFD) for HP4M mold steel. With only two extreme cases of this parameter in DOE analysis, it

will only reveal the main effect in the representation of two points. Instead, by introducing a few more abrasive sizes, the curves on the graph may not be a linearly straight line.

2. Introducing the processing time as a parameter into the DOE analysis is necessary to optimize MAF processing efficiency.

3. The effect of the weight or volume fraction of silicone oil will also be investigated as it influences the viscosity and stiffness of the MAF brush. So far the experiment introduced two different weight fractions of silicone oil in an MAF brush. A concrete conclusion should be drawn by varying the weight fraction of silicone oil which enables to carry out a more thorough study of the impact of stiffness of the MAF brush.

CHAPTER 3: CONTINUOUS SETUP FOR THE LARGE AREA FINISHING BY MAF PROCESS

3.1 Introduction

Magnetic-field Assisted Finishing (MAF) is a relatively new surface finishing technology, which garnered significant attention for its remarkable ability to achieve mirror-quality surfaces for various materials using well-established CNC technology. However, its main applications primarily lie in the field of optical [52-54] and soft material finishing such as copper [55-58]. The applications of MAF could be broadened to be applicable in many modern industrial metal surface finishing cases. One of the most interesting materials is sheet metal products manufactured by Arcanum Alloys (Kentwood, Michigan), and the processes of fabricating the coating layer of sheet metal and post-processing are shown in Figure 3.1, following the order of the arrows. The substrate metal used in this process was composed of interstitial-free (IF) steel, which is a type of low-carbon steel. To create the substrate, a thick slab was cold rolled to form a thin 1 mm foil. Next, a specialized slurry containing chromium (Cr) that functions to improve the hardness and corrosion resistance was continuously applied onto the surface of the sheet substrate. Subsequently, the slurry-coated coil underwent annealing in a controlled atmosphere at elevated temperatures. During this annealing process, the chromium particles within the slurry vaporized, migrated, and diffused into the underlying base metal substrate. In the post-process, the sheet metal was cleaned. However, the main barrier to this technique was that the coating process generated a non-uniform surface aesthetic, which was not easy to finish exterior surfaces with currently available processing techniques. Therefore, it is necessary to incorporate some other surface finishing techniques such as the MAF process into this production process. The implementation of a continuous MAF system is crucial for achieving efficient completion of large areas while ensuring seamless integration with pre-existing infrastructure. Our innovative module of the continuous MAF setup, as shown in the fifth step in Figure 3.1, is designed as a drop-in-cell system, offering seamless integration with any sheet metal production line without requiring significant modifications. This remarkable feature makes it highly appealing to metal plating and finishing companies such as Pioneer Metal Finishing, Anoplate Corporation, SPC, and others, as well as sheet metal production companies like Combined Metals of Chicago, AK Steel Holding, and more. The financial impact in terms of capital expenditure is bound to impress these industry players.

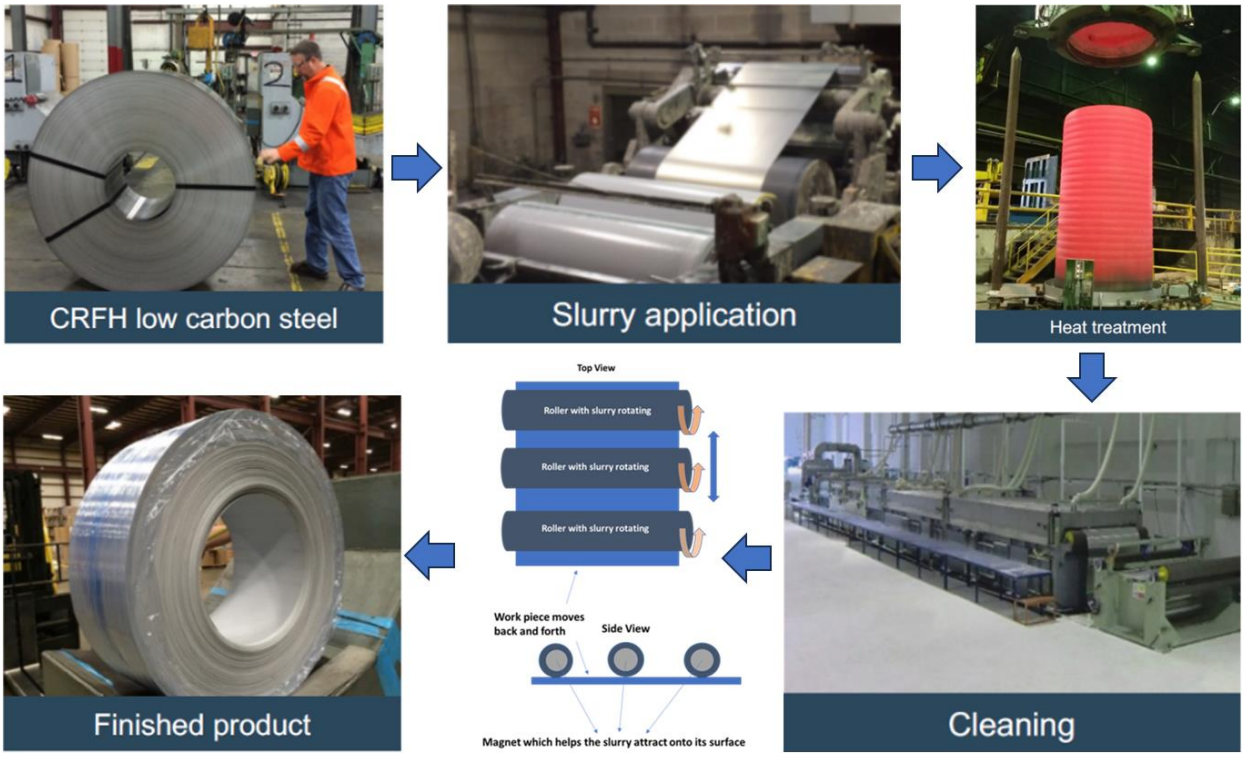

Figure 3.1: Manufacturing processes of producing a coating layer of sheet metal with the implementation of the MAF process

3.2 Objectives

The primary objective of this study was to design a continuous setup to finish the surface of chrome-coated sheet metal by the MAF process by introducing the optimal processing parameters from section 2.4 and evaluating the surface finish on large area of the sheet metal. The experimental setup must be designed so that any industry could implement it to finish the coated surface of sheet metal. Hence, a specifically designed MAF setup was developed to work in a continuously producing sheet metal environment.

3.3 Experimental Setup

The schematics of the continuous setup for sheet metal product is shown in Figure 3.2.

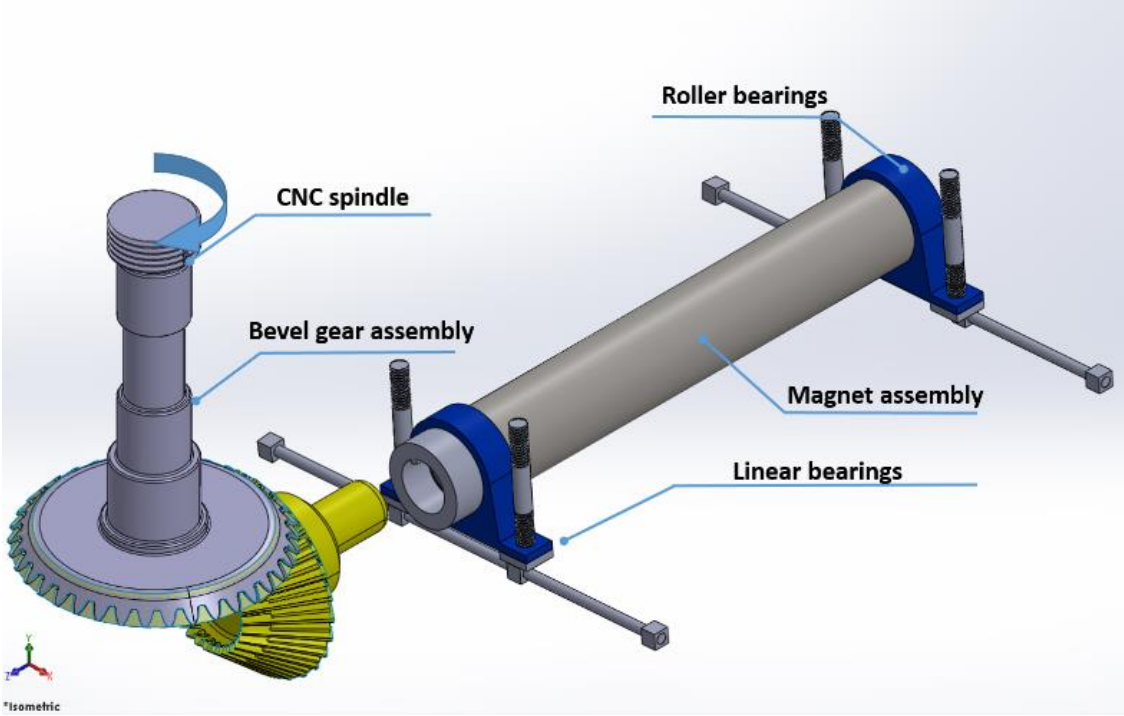

Figure 3.2: The schematic of the continuous setup

A traditional CNC milling setup was used to finish the sheet continuously. The major components of the setup are magnet assembly, roller bearings, linear bearings, and the bevel gearbox. The bevel gearbox is employed to alter the rotational direction, allowing for the arrangement of a set of magnets in the magnet assembly. These magnets generate a magnetic force that acts upon the MAF brush, enabling horizontal polishing of the workpiece. As shown in Figure 3.3, one end of the bevel gear assembly is mounted to the CNC spindle, and the other end is attached to the aluminum rod which holds a stack of 30 ring-shaped magnets stacked outside this aluminum rod. This assembly of aluminum rod and magnets is illustrated in Figure 3.3. The aluminum rod is held between two roller bearings and connected to the bevel gear. As the CNC spindle rotates, the aluminum rod containing a series of magnets rotates with the MAF brush on the exterior surface of the magnet assembly while polishing a wide area of the sheet metal sample. The roller bearing is then connected to a linear bearing using an anchor plate. Linear bearing rails are connected to the CNC carriage as shown in Figure 3.3. The linear movement in the CNC carriage moves the workpiece while keeping the magnetic assembly setup stationary. The current setup is capable of polishing up to 200 mm wide and 600 mm long sheet samples. Further, this continuous MAF setup is compatible with our CNC milling machine. The dimensions of the current setup are constrained because of the current working space of our CNC milling, but the primary advantage of this setup

was that it could easily be scaled up to finish large sheets in an industrial production environment. A longer magnet assembly would increase the width of the polishing area, and a wider CNC carriage could accommodate longer sheet samples.

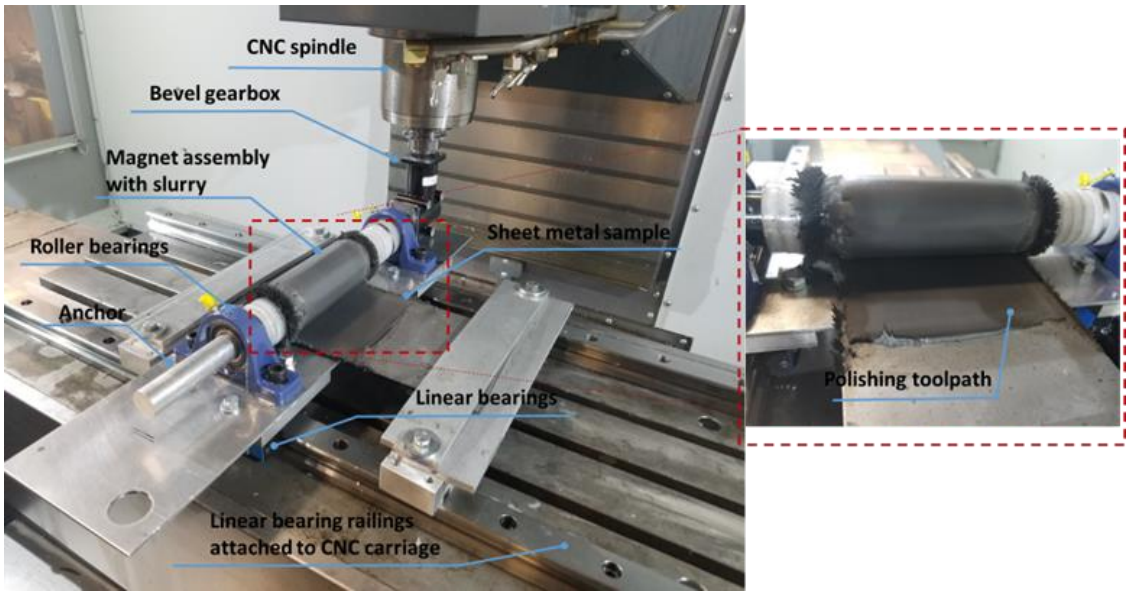

Figure 3.3: Continuous setup for MAF process on polishing wider samples of chrome-coated low carbon steel sheet metal

3.4 Preparation of MAF Brush and Workpiece Material

The brush was made of BC particles (with an average size of 3 μm from Beta Diamond Products; Yorba Linda, CA) and iron particles (with an average size of 150 μm from Carolina Biological Supply Company; Burlington, NC) mixed with silicone oil (DM-1,000,000 CGS from ShinEtsu; Akron, OH). The large chrome-coated sheet was the same material that was mentioned in section 2.4.3 and the optimal brush composition was determined in section 2.4.5 to be a 4:1:1.5 weight ratio in terms of iron particles, BC, and silicone oil. Other specific optimal processing parameters can be found in Table 3.1 which are the same processing conditions from section 2.4.5.

Table 3.1: Optimum processing parameters for polishing sheet metals with MAF

Parameters	Optimum value
Abrasive	Black ceramic
Abrasive size	3 μm
Brush composition	4:1:1.5 (Iron:BC: Silicone)
Finishing time	2.5 hours
Spindle speed	600 RPM
Feed rate	3.1 in/min
Gap distance	2 mm

3.5 Result and Discussion

As the optimum processing parameters were determined with our standard MAF setup on smaller sheet samples, it was necessary to replicate similar results in the designed continuous setup.

The surface roughness measurements, before and after the MAF process, were obtained from the continuous setup as shown in Figure 3.4. The final surface roughness values achieved were 220 nm and 405 nm from two chrome-coated large sheet samples with the initial surface roughness of around 2370 nm and 3100 nm, respectively. The final surface roughness values, however, of the large sheet samples polished with continuous setup were not as well polished as the one with the smaller setup that was used to find optimum processing parameters, as compared to Figure 2.15 and Figure 3.4. This could be a result of different magnetic field orientations and flux densities between the two setups. In the smaller setup, the magnetic field is normal to the workpiece sample whereas the magnetic field is in the parallel direction in the continuous setup. Also, the magnetic flux density (measured by PCEMFM 3500 - PCE instruments, Jupiter, FL, USA) of the small-scaled setup was 408 mT whereas the magnetic flux density for the continuous setup was only 130 mT. The magnetic flux density directly affects the normal and shear force applied on the workpiece during the surface finishing process which in turn affects the material removal rate and the final surface roughness of a part. This magnetic field orientation effect should be considered and studied further in the future. Figure 3.5 shows the dramatic difference between the initial surface and final surface quality. The clear reflection image on the final surface after MAF illustrates that the

polished area has become a mirror-like surface whereas the images could not reflect the image from the initial rough surface.

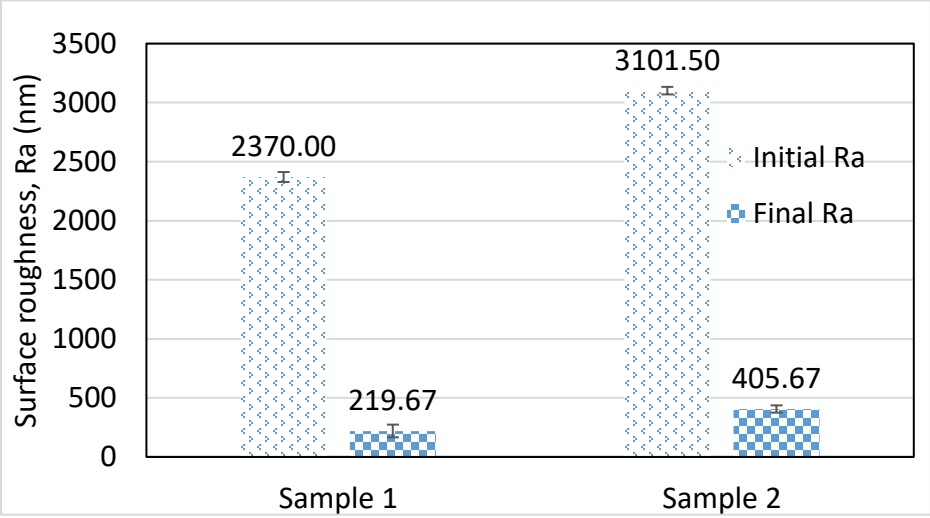

Figure 3.4: Surface roughness comparison before and after MAF on sheet metal with continuous MAF setup

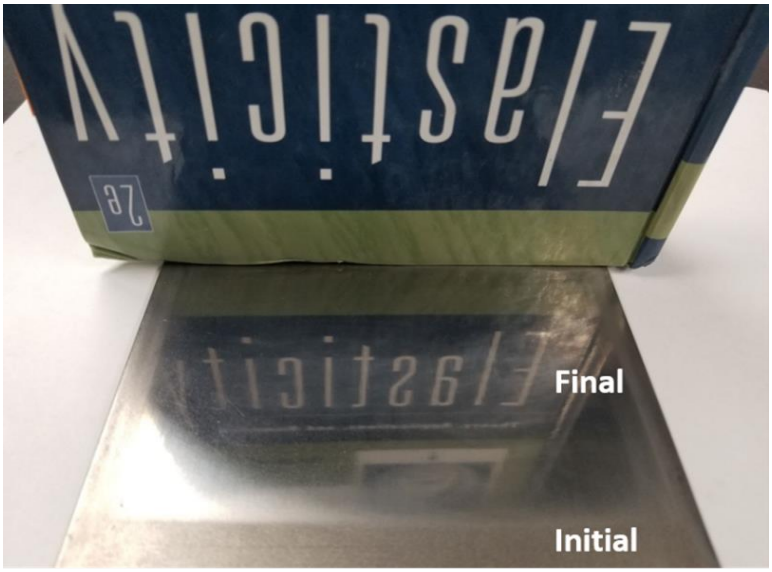

Figure 3.5: Reflection image comparison before and after MAF on sheet metal with continuous MAF setup

3.6 Conclusion

In this study, chrome-coated steel sheet samples were polished using two different MAF setups. The optimum processing parameters were achieved for finishing sheet metal samples using the small-scaled setup, then those parameters were applied to the continuous setup for surface finishing the larger area of sheet metal samples which increases the effectiveness and efficiency of the

finishing process. The mirror-like surface finish demonstrated the optimal processing parameters could be implemented from the small-scaled setup to the continuous setup within 2.5 hours. The continuous setup can also be scaled up even more as required and can eventually be easily integrated into the continuously produced sheet metal environment which is the biggest advantage of this experimental setup.

CHAPTER 4: FUNDAMENTAL STUDY ON MAF BRUSH CONSTITUENTS

4.1 Introduction

In studying MAF, the constituents of the brush used in the process are important factors to make MAF more effective because they directly interact with the workpiece surface and carry the abrasive particles during the finishing process. As mentioned earlier, the brush constituents normally include ferromagnetic and abrasive particles within a viscous medium. The ferromagnetic particles, typically iron or carbonyl iron particles (CIPs), are suspended within a liquid medium and respond to the magnetic field due to their magnetic properties. They align themselves along the magnetic field lines, forming chains or columns and the extent of columns is dependent on the strength of the magnetic field. The abrasive particles, such as silicon carbide (SiC) or diamond, embedded within the magnetic abrasive slurry contribute to the cutting and grinding action on the workpiece surface. These particles have sharp edges that facilitate the removal of material by abrasion. Therefore, the selection and characteristics of brush constituents can significantly influence the material removal rate, surface quality, and overall performance of the MAF process.

In the past decades, researchers have dedicated significant efforts to examining the constituents of MAF brushes. These investigations have addressed various aspects of MAF, including the brush composition, the sizes of ferromagnetic and abrasive materials, as well as the volume or weight ratio, and so on. Jain et al. [59] discovered that the percentage improvement in Ra value increased with the increase in abrasive concentration. Sidpara et al. [60] emphasized the significant impact of the base medium of the MAF brush and highlighted that an oil-based brush exhibited lower yield stress compared to a water-based brush under an applied magnetic field. This lower yield stress weakened the brush's strength. Guo et al. [61] concluded that the surface roughness and surface morphologies were mainly affected by the type and size of the abrasives. They found that SiC-based abrasives outperformed alumina-based abrasives, resulting in a higher material removal rate. To validate the material removal rate model, Kum et al. [62] experimentally verified it by varying the abrasive size and abrasive concentration. They observed a decrease in material removal rate with an increase in abrasive size. Additionally, the material removal rate initially increased, reaching a maximum at an abrasive volumetric concentration of 25.9%, and then decreased with an additional increase in the abrasive volume ratio. Hashmi et al. [63] also confirmed that surface

roughness decreased with increasing volumetric abrasive concentration up to an optimum level of 20%. Beyond this threshold, roughness increased due to the weakening of iron particle chain-like structures caused by the increased volume percent of abrasive particles. Khan et al. [29] identified the abrasive size as the most important parameter, followed by iron powder concentration and abrasive concentration. They determined that increasing the iron content enhanced the finishing effect in terms of a higher percentage change in surface roughness value. The optimal brush composition was found to be 14% of abrasive particles and 25% iron particles with the rest content of base fluid in terms of volumetric percentage. Furthermore, Hitomi et al. [64] applied MAF to the internal finishing process and reported the highest material removal was obtained in the case of the largest iron particles since it provided the greatest magnetic force. Despite numerous studies on MAF brush constituents, the explanation of the size effect of iron and abrasive remains vague, with limited supportive data or explanations available in recent literature. This study aims to provide a comprehensive analysis of MAF brush constituents through experiments and simulations.

4.2 Objectives

The objectives of this study are to:

- Find the optimal size variation of the abrasive and determine the impact of different sizes of abrasive particles on the MAF process
- Optimize the processing time of MAF regarding different sizes of abrasive particles to evaluate the efficiency of the MAF process
- Determine the optimal size of iron particles and the relationship between different sizes of iron particles and abrasive particles
- Focus on fundamental studies of brush constituents to explain the phenomenon of the combination of larger iron particles and smaller abrasive particles enabling a better surface finish

4.3 Materials and Methods

4.3.1 Workpiece and Experimental Setup

The workpiece is made of AISI S7 steel with dimensions of 40x40x10 mm, as shown in Figure 4.1. The customized magnet tool holder was fabricated with a 0.5-inch diameter and this magnet tool was mounted onto the spindle of the HAAS VF-4 CNC milling machine, as shown in Figure 4.2.

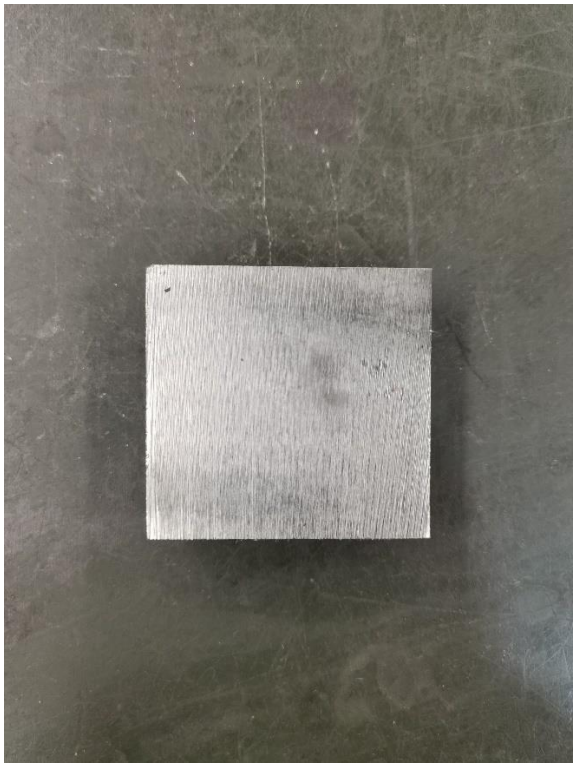

Figure 4.1: Dimension by 40x40x10 mm AISI S7 steel

Figure 4.2: Experimental setup of magnet tool and AISI S7 steel workpiece

4.3.2 MAF Brush Preparation

The optimal processing parameters of the MAF process were found in the previous section and conclusive parameters can be found in Table 4.1. The selected abrasive type was BC with ferromagnetic particles made of iron. The experimentation involved a wide variety of sizes of both BC and iron, depending on the specific objectives of the study. Brush composition was determined to be in the weight ratio of 4:1:1.5 for iron, BC, and silicone oil, respectively. The processing conditions for the machine setup, including gap distance, feed rate, and rotational spindle speed were 2 mm, 3.1 inches/minute, and 2000 RPM, respectively.

Table 4.1: Selective and optimal processing parameters for MAF on AISI S7 steel

Parameters	Optimum value
Abrasive	Black ceramic (BC)
Ferromagnetic Particle	Iron
Brush composition (by weight)	4:1:1.5 (Iron:BC: Silicone oil)
Gap distance	2 mm
Feed rate	3.1 in/min
Spindle speed	2000 RPM

4.4 Results and Discussions

4.4.1 Size Variation of BC Influence Surface Roughness

In this experimental study, the average BC sizes ranging from 3 to 75 μm were introduced into iron particles of a single size (200 μm), as outlined in Table 4.2.

Table 4.2: Table of different experiment

BC size (μm)	Iron size(μm)	Processing conditions:
3	200	Spindle speed: 2000 RPM Feed rate: 3.1 in/min Gap distance: 2 mm Passes: 25
10		
13		
30		
75		

The results indicate a decrease in surface roughness as the MAF process proceeded, as shown in Figure 4.3. It is important to note that the MFA brush traverses the workpiece surface, and each complete back-and-forth movement is considered a single pass. Within 25 passes, a significant improvement in surface roughness was achieved, reaching values as low as 0.1 μm. This corresponded to approximately 96% enhancement using the smaller average sizes of BC, 3 and 10 μm. Conversely, when the average BC size exceeded 30 μm, the improvement in surface finish dropped to around 50% or even lower. Additionally, an interesting observation was that the behavior of the surface roughness curve differed based on the size of the BC particles used. When smaller BC sizes were employed, the curve decayed in an exponential fashion while larger BC sizes decayed in a linear fashion. Moreover, the 13 μm BC appeared to act as a threshold between the linear and exponential decay behaviors. However, a more desirable scenario involves a reduced average BC size, as this corresponds to a greater quantity of smaller abrasives compared to larger ones. Consequently, using a greater quantity of smaller abrasives enhances their involvement in the finishing process. This approach facilitates the removal of surface imperfections in fewer passes, resulting in lower energy consumption while achieving efficient surface finishing.

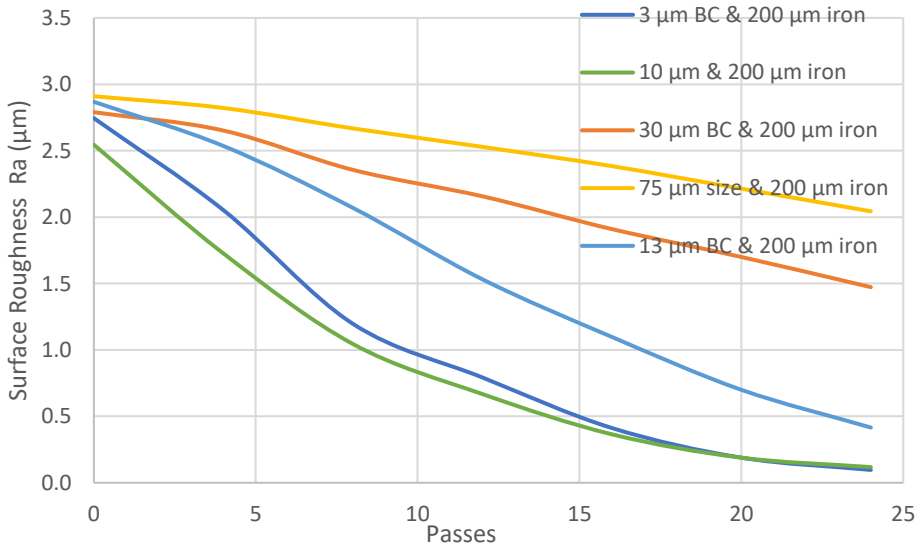

Figure 4.3: Surface roughness over short traversing passes (up to 25) of the brush on S7 steel with different sizes of BC

4.4.2 Optimization on MAF Finishing Time or Passes

Subsequently, another experiment was performed to explore the minimal passes for the MAF process while limiting the iron particle size to 200 μm. In this experiment, a wider size range of

BC was used compared to the previous study, and additional passes were implemented to observe the subsequent behavior in more detail. These parameters are shown in Table 4.3.

Table 4.3: Table of different experimental conditions

BC size (μm)	Iron size(μm)	
3	200	Processing conditions: Spindle speed: 2000 RPM Feed rate: 3.1 in/min Gap distance: 2 mm Passes: 120
30		
125		
600		
850		

This experiment used a brush made of various sizes of BC (from 3-850 μm) and maintained a consistent size of iron particles at approximately 200 μm. The objective was to observe the minimal number of passes that the MAF process could achieve under different conditions, as shown in Figure 4.4.

Initially, it was observed that using BC sizes of 3, 30, and 125 μm resulted in a significant improvement in surface finish with less than 120 passes. However, larger BC sizes (600 and 850 μm) did not lead to further improvement as the MAF process continued. Moreover, it was found that the smaller the BC size, the fewer passes were needed to achieve surface improvement. For instance, using the 3 μm BC, the surface improvement reached approximately 90% after around 26 passes. In comparison, achieving a similar result with 30 μm BC would require approximately 60 passes. Conversely, when the BC size increased to 125 μm, the surface improvement could not reach 90% even after 120 passes.

Based on these findings, it can be concluded that decreasing the BC size led to better surface improvement. The minimal number of passes was determined to be 26 with the smallest BC size (3 μm). It is not recommended to increase the number of passes beyond this point to achieve better surface finishing, as the economic production cost would outweigh the marginal improvement of less than 5% obtained by doubling the number of passes.

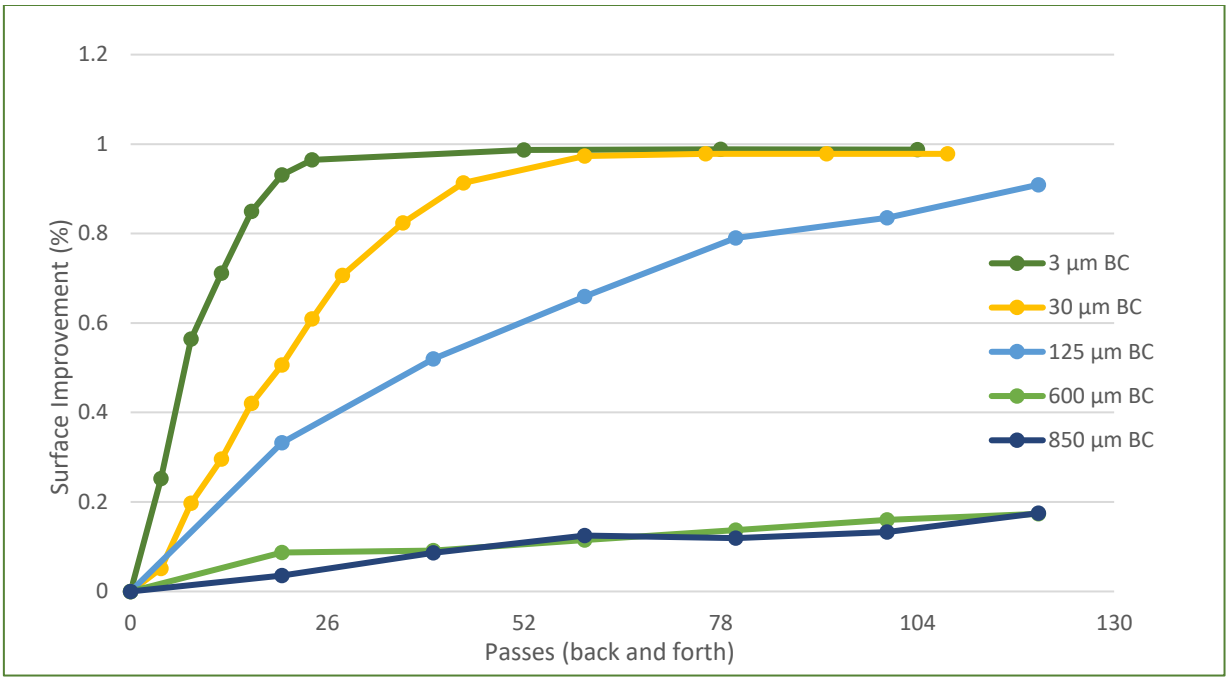

Figure 4.4: Surface roughness over long traversing passes (up to 120) of the brush on S7 steel with different sizes of BC

4.4.3 Optimal Size Variation of Iron Particles

Iron size also plays a crucial role in determining the performance of the MAF process. Iron particles serve as the foundation to form a chain-like structure and act as a carrier matrix to retain the abrasive particles needed for the MAF process. To assess the impact of surface finish quality, an additional experiment was conducted using other iron sizes in conjunction with different BC sizes as shown in Table 4.4, that each BC size will consecutively experiment with different iron sizes.

Table 4.4: Table of different experimental conditions

BC size (µm)	Iron size(µm)	Processing conditions: Spindle speed: 2000 RPM Feed rate: 3.1 in/min Gap distance: 2 mm Passes: 120
3	40	
10	150	
75	200	
125	400	
N/A	800	

The influence of iron particle size on the surface finish is critical, which is evident based on Figures 4.5 to 4.8. Irrespective of the specific conditions involving different sizes of BC, the presence of larger iron particles consistently led to greater surface improvement. The most notable enhancements in surface quality were achieved when utilizing the iron particle sizes of 800, 400, and 200 μm. Particularly, when two smaller BC sizes (3 and 10 μm) were employed, the surface roughness could be reduced to below 100 nanometers, aligning with expectations based on the positive impact of smaller BC on surface finishing demonstrated in Sec. 4.4.1. However, noticeable surface improvements were not observed in the cases when larger BC (75 and 125 μm) were used, especially when the size of the iron particle was below 200 μm, as illustrated in Figures 4.7 and 4.8. This phenomenon may be attributed to the larger BC leading to increased spacing between iron particles, thereby reducing the interaction force necessary for securely holding the abrasives. This effect can be considered analogous to that the iron particle chain-like structures are being compromised due to the higher percentage of abrasives, resulting in their diminished magnetic strength, as reported by Hashmi et al. [63].

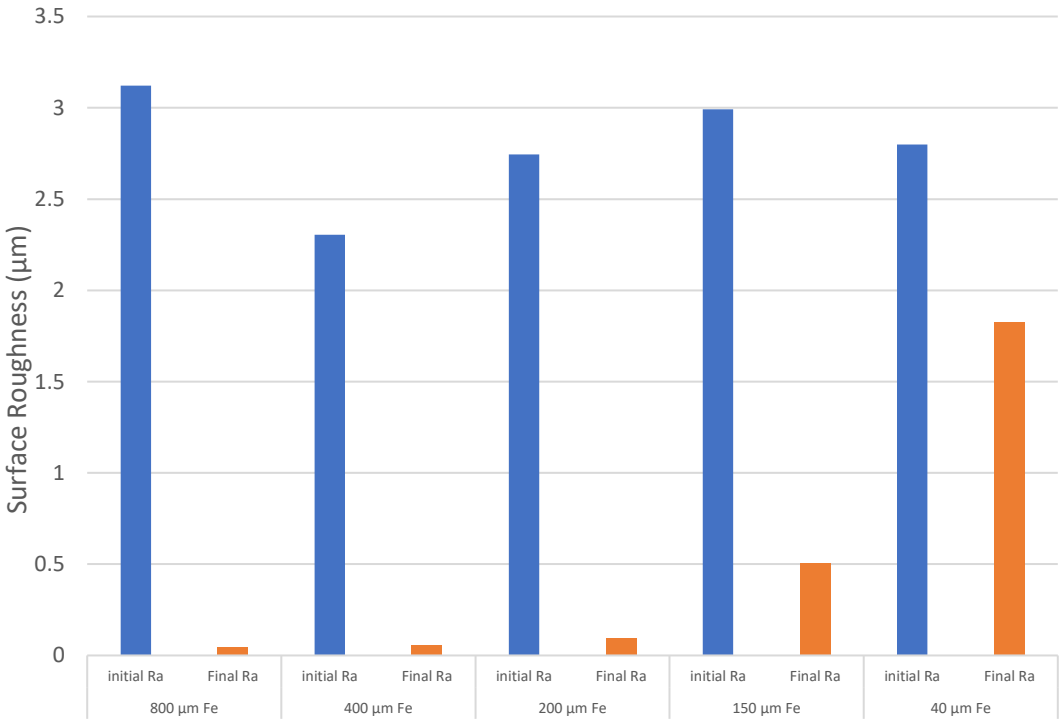

Figure 4.5: Surface roughness over different sizes of iron with 3 μm size of BC

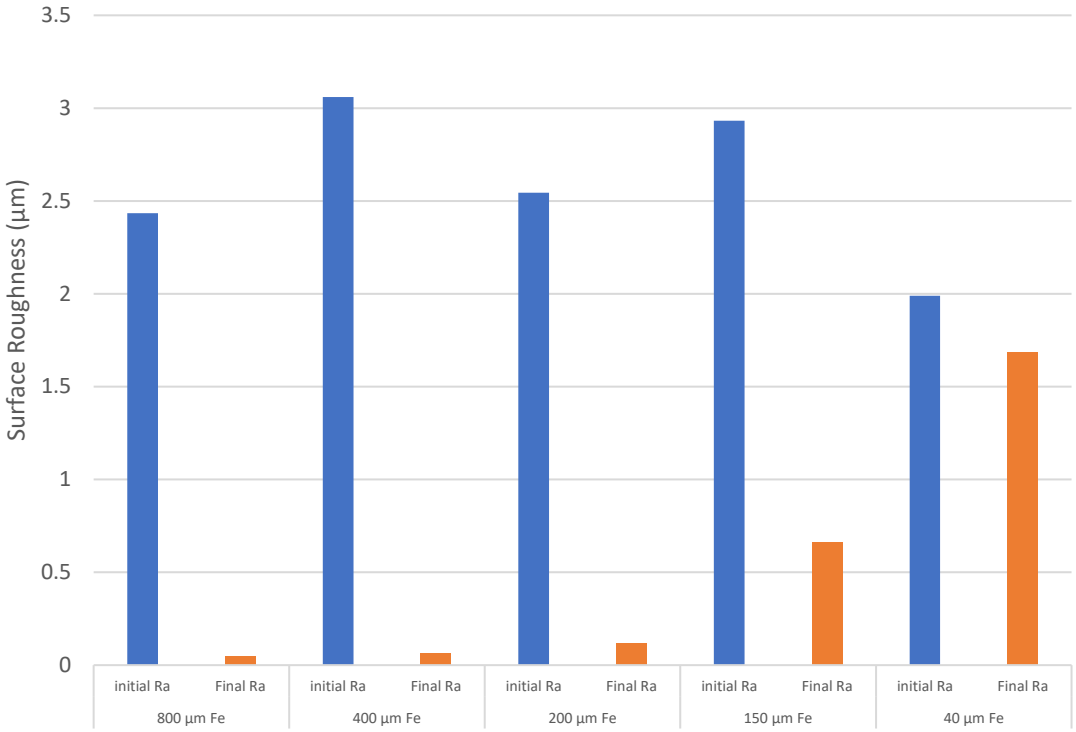

Figure 4.6: Surface roughness over different sizes of iron with 10 µm size of BC

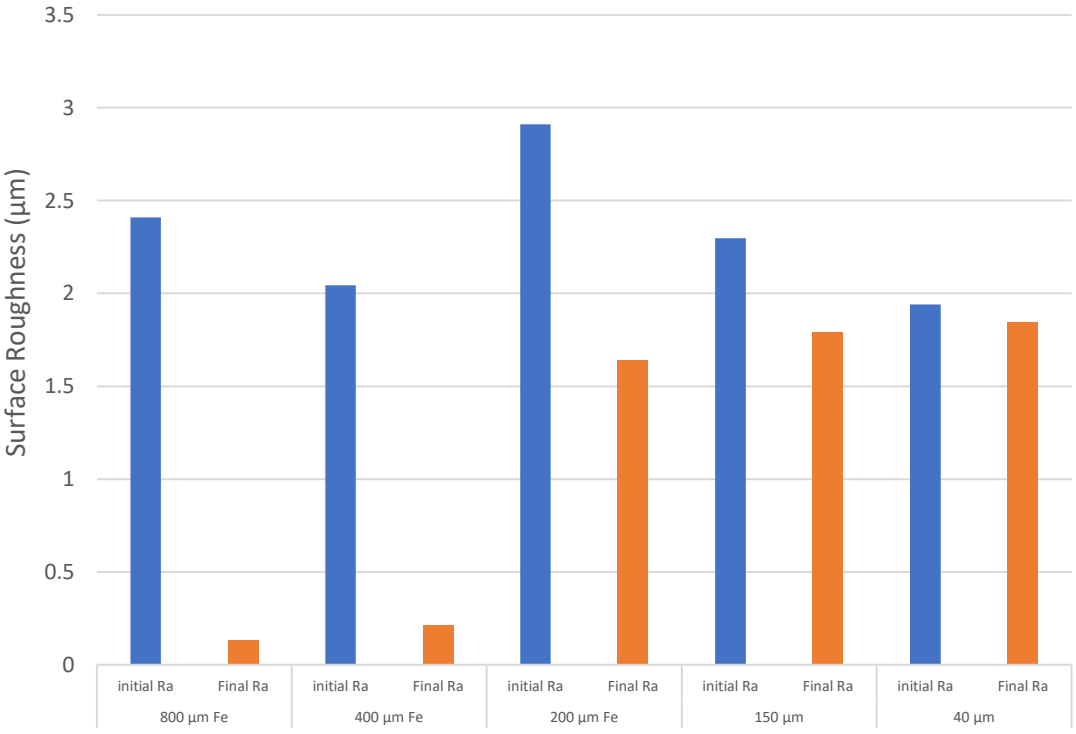

Figure 4.7: Surface roughness over different sizes of iron with 75 µm size of BC

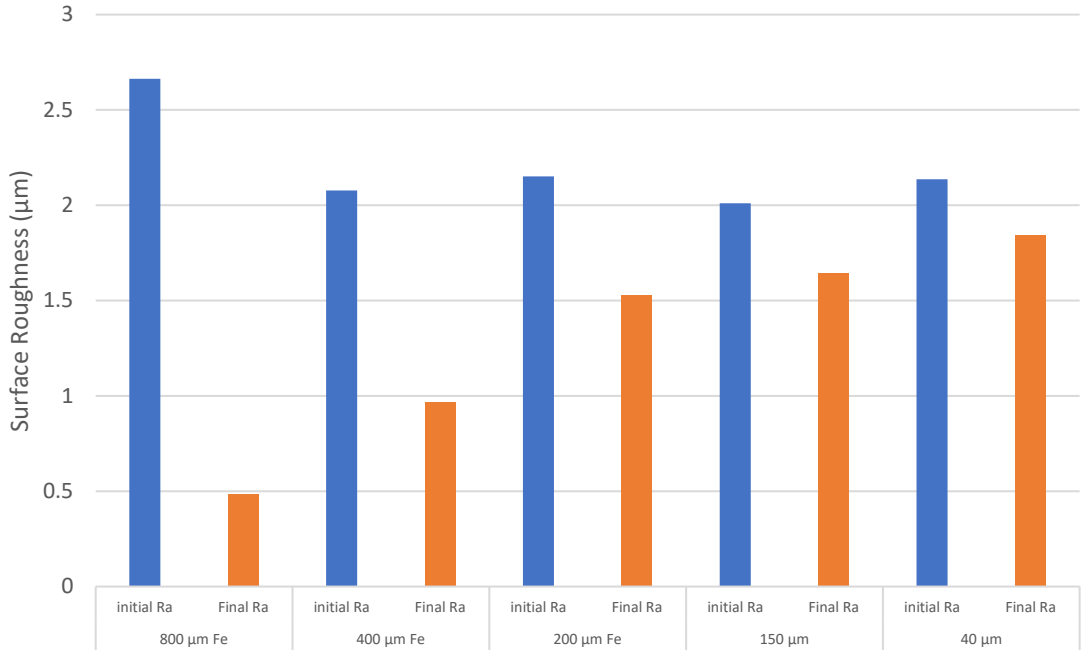

Figure 4.8: Surface roughness over different sizes of iron with 125 µm size of BC

4.4.4 Fundamental Study on Brush Constituents

In the preceding experimental study, a recurring observation was the consistent improvement in surface finish and material removal as the brush with larger iron particles and smaller sizes of BC improve the MAF performance. In order to delve into the underlying mechanism behind this phenomenon, additional experiments were conducted.

Table 4.4: Table of different experimental conditions

BC size (µm)	Iron size(µm)	Processing conditions:
3	200	Spindle speed: 2000 RPM Feed rate: 3.1 in/min Gap distance: 2 mm Passes: 26
560		

To provide visualization of the brush before and after the MAF process, two additional experiments were conducted using different sizes of abrasive particles in combination with the 200 µm iron particles. Specifically, a smaller BC (3 µm) and a larger BC (560 µm) were employed, as indicated in Table 4.4. Both experiments were conducted in identical conditions for over 26 passes.

A notable distinction in the appearance of the MAF brush was evident compared to the images presented in Figures 4.7 and 4.8. This disparity resulted from the grayish color of the 3 μm BC, which led to a greater number of these BC particles being embedded in the MAF brush. Notably, the larger BC particles (560 μm), as shown in Figure 4.9, were repelled away from the brush center. However, when the 3 μm BC was used, as evident in Figure 4.10, there was less segregation of the MAF brush both before and after the MAF process. The 560 μm BC particles were too large to be securely held due to the centrifugal force at the center of the MAF brush, which is the region responsible for efficient grinding as it directly contacts the surface of the workpiece under the maximum magnetic force. Consequently, smaller abrasives yield a superior surface finish since they can be easily embedded in the MAF brush without being repelled away due to the centrifugal force applied on each smaller abrasive.

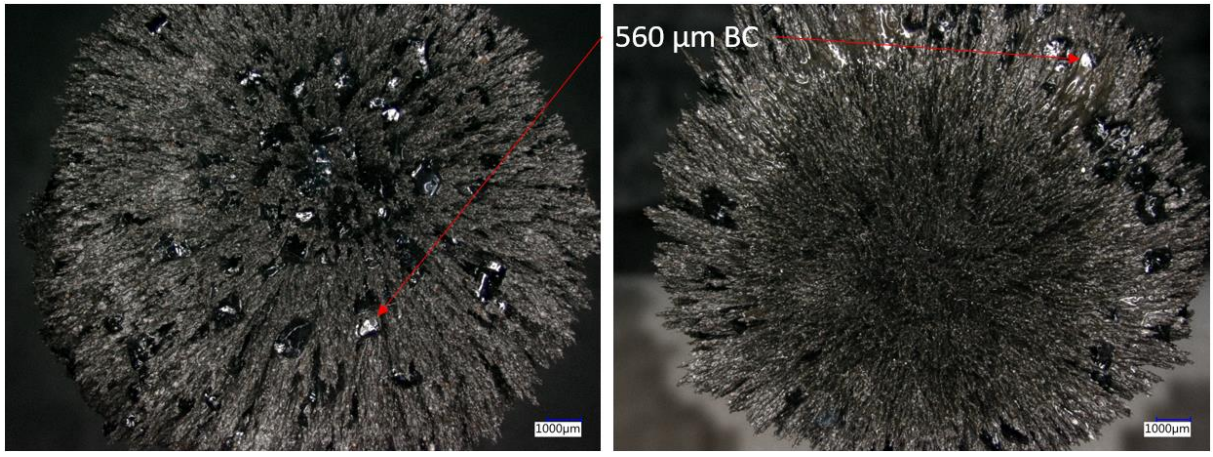

Figure 4.9: Optical image of brush with 200 μm iron size and 560 μm BC size before (Left) and after (Right) after the MAF process for 26 passes

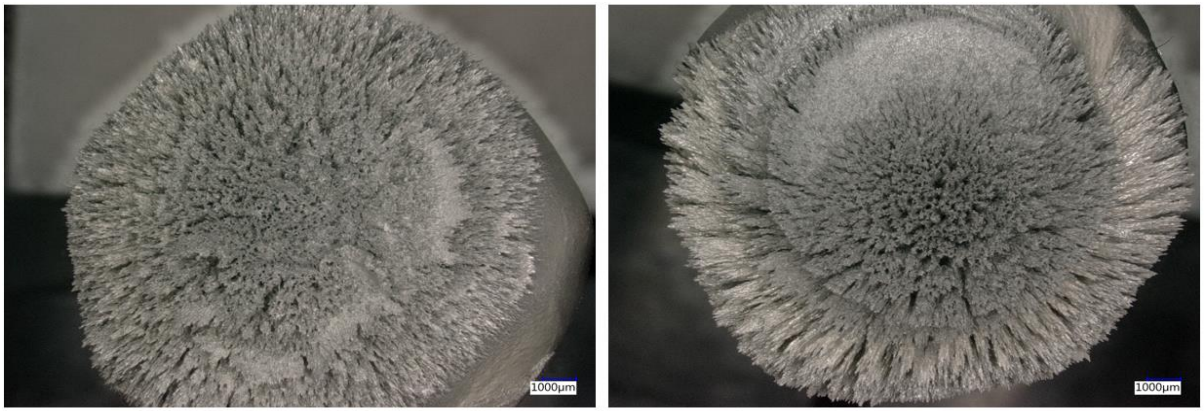

Figure 4.10: Optical image of rush with 200 μm iron size and 3 μm BC size before (Left) and after (Right) after the MAF process for 26 passes

Moreover, it is essential to conduct a thorough examination of the efficacy of ferromagnetic particles (iron in this study) in the MAF process. This investigation is crucial because iron particles directly interact with the abrasive material and exert both normal and shear forces on the workpiece. To gain a deeper comprehension of the behavior of iron particles, it becomes necessary to introduce the concept of magnetic flux density (MFD), which represents a fundamental parameter in magnetic analysis. MFD pertains to the strength or intensity of a magnetic field at a particular point in space. It represents the amount of magnetic flux passing through a given area per unit area.

It can be seen that the Gauss meter measurements among the brushes consisting of different iron particle sizes but equal weight show almost identical magnetic flux densities as shown in Figure 4.11. This also implies that the large iron particles, because it contains fewer number particles, possess a greater capacity to absorb magnetic flux per unit of surface area compared to the small iron particle. Consequently, large iron particles can be magnetized to a greater level than smaller ones and it causes more interactive magnetic force among large iron particles, enabling the column structures to firmly grasp abrasive particles. Further explanation of the simulation on iron particles with different sizes will be provided in the subsequent discussion.

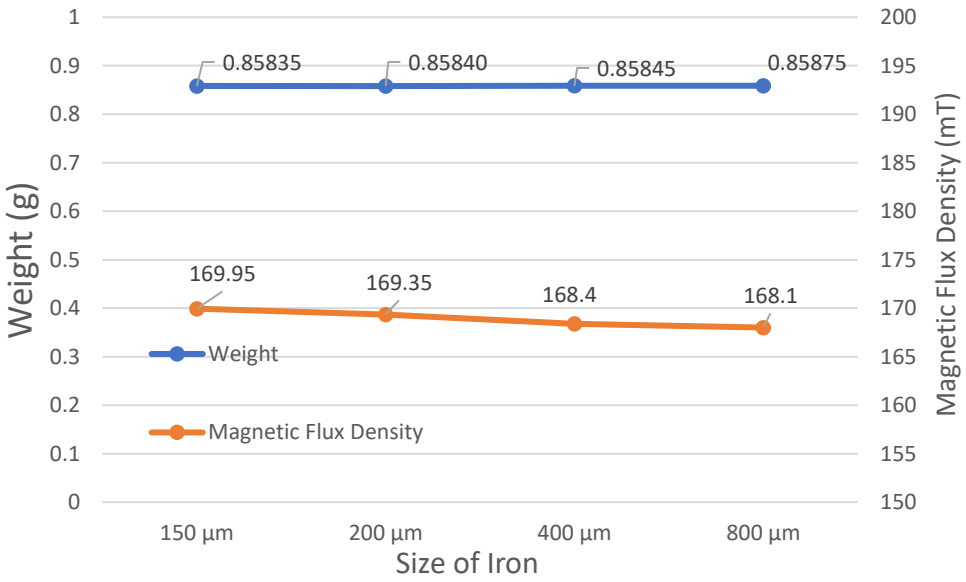

Figure 4.11: Weight measurements and received magnetic flux density for different sizes of iron particles

Simulation Set-up

The ANSYS Workbench and Magnetostatic Module were used to simulate the magnetic force between different sizes of iron particles. To simplify the simulation model, all iron particles were

treated as spheres. The diameter of the ball magnet was assumed to be 0.5 inches (12.7 mm), and such a system was encompassed by an enclosure. The enclosure defines the boundaries of the simulation domain. It provides a closed region in which the magnetic field is analyzed and how the magnetic field interacts with the surroundings, as shown in Figure 4.12.

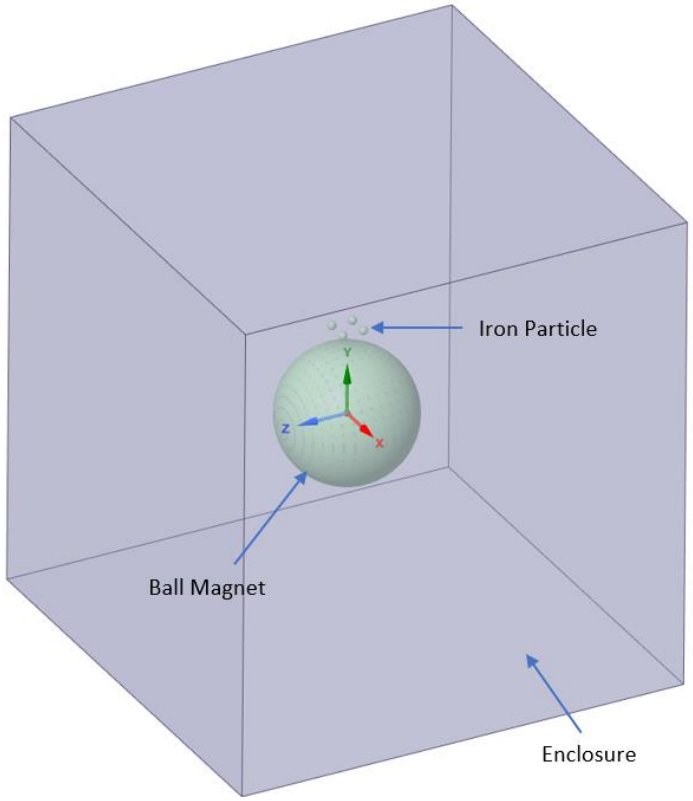

Figure 4.12: Geometry design of the iron particles and ball magnet simulation

The initial condition was set as the magnetization of the ball magnet which was considered to be a permanent magnet. Furthermore, the element shape was set to be quadratic to achieve higher accuracy and a more precise representation of the magnetic field distribution within the simulated region, as shown in Figure 4.13. Quadratic elements, also known as second-order elements, provide a higher degree of interpolation compared to linear elements, resulting in a more detailed and refined mesh. The element size was 0.5 mm for the ball magnet and 0.1 mm for the iron particle to improve the result.

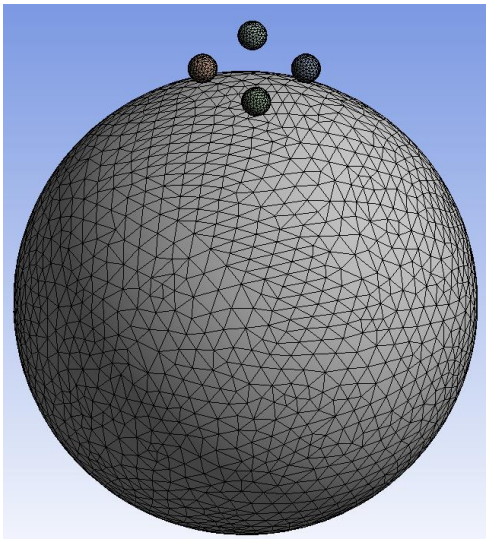

Figure 4.13: Mesh condition shows the quadratic element shapes of the simulation

Result and Discussion

The simulation allows us to estimate the magnetic force resulting in each single iron particle since the magnetic force between two adjacent iron particles can be directly correlated, enabling them to place the abrasives among them. The magnetic force was simulated for different iron sizes, where the total weights of the iron particles in two different scenarios are the same, as shown in Figure 4.14. The Cartesian coordinate system represented Y and Z directions (lateral) in the green and blue arrows, respectively.

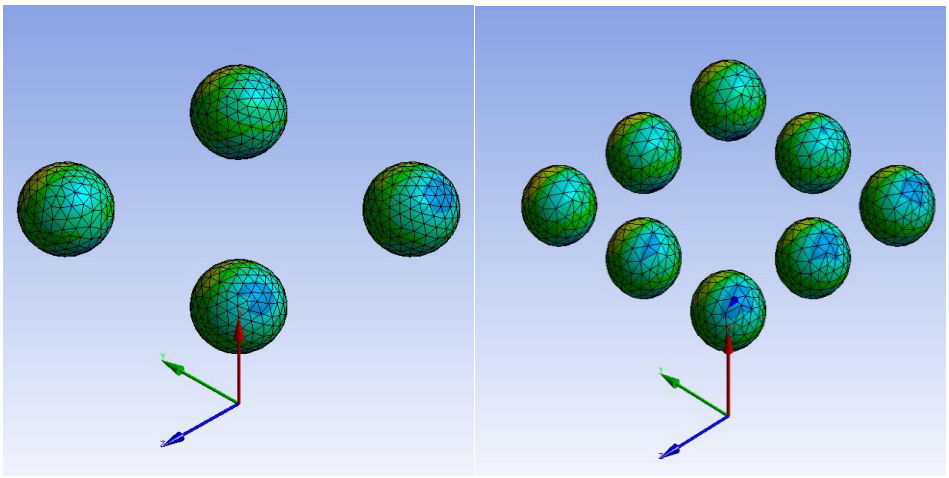

Figure 4.14: Demonstration of magnetic force simulation for 4-iron particle case (Left) and 8-iron particle case (Right)

From the simulation result presented in Table 4.5, the individual large iron particle in the 4-iron particle case experienced a lateral magnetic force of 0.0173 N, which was higher compared to the

individual small iron particle in the 8-iron particle case. This observation supported the previous findings (in Figure 4.11) that a single larger iron particle facilitated increased magnetization due to its larger surface area. Consequently, the larger iron particle is subjected to a greater magnetic force resulting in the formation of robust chain-like structures that exhibit a two-body abrasion mechanism, providing enhanced processing capability. This mechanism allows the sturdy chain-like structures to securely grip the abrasive particles, thereby facilitating a sliding motion between the abrasive particles and the surface of the material. Conversely, the smaller iron particles experience comparatively weaker magnetic forces between them, enabling them to roll freely, resulting in a three-body abrasion mechanism. In this process, the absence of external forces acting on the material surface by the loose abrasive particles results in a reduced finishing efficiency.

Furthermore, the total magnetic force presented in the 8-iron particle case surpassed the total magnetic force in the 4-iron particle case. This disparity arose from the fact that the smaller iron particles possessed a larger overall surface area, resulting in a stronger total magnetic force exerted on them. However, this does not imply that the force experienced by the chain-like structures formed by the smaller iron particles is greater. In fact, the magnetic force between two adjacent smaller iron particles is smaller, leading to a reduced interaction force within the chain-like structure, and the limited strength within the interconnected chain structures created by the smaller iron particles still leads to the occurrence of the three-body abrasion as the main mechanism.

Table 4.5. Comparison of force for large and smaller iron particles on individual and groups of iron in the lateral direction

The YZ-plane force of individual iron (Newton-N)	4-iron particle case	8-iron particle case
Directional force (Y)	0.0117	0.00895
Directional force (Z)	0.0127	0.00907
Total	0.0173	0.0127
The YZ-plane force of groups of iron (Newton-N)	4-iron particle case	8-iron particle case
Directional force (Y)	0.0111	0.0202
Directional force (Z)	0.00985	0.0133
Total	0.0148	0.0242

4.5 Conclusion

The study focused on developing a systematic methodology to determine the optimum processing conditions related to abrasive particle size, iron particle size, and traversing passes (processing time). The findings of the study enable us to examine the constituents of the brush to improve the efficiency of the MAF process. The study yielded the following specific conclusions:

- With the fixed iron particle size, it was found that smaller BC was more effective in providing an impressive 96% enhancement in surface finishing, which was achieved with the 3 μm BC in the brush.
- With decreasing BC size, the number of passes required for superior surface improvement decreased as well, reducing processing time. For instance, with the 3 μm BC in the brush, the surface improvement reached approximately 90% after running 26 passes.
- Choosing a larger iron particle size in the brush contributed to a better surface finish. However, as the abrasive size increased, the performance was diminished.
- The fundamental study of the MAF brush, aided by the simple simulation work, provided an explanation for why larger iron particles and smaller abrasives resulted in superior surface finishing. The brush with the increased iron particle size leads to a stronger magnetic force acting upon it, leading to the creation of robust chain-like structures that exhibit the two-body abrasion mechanism, thereby improving the processing capacity. On the other hand, the diminished magnetic forces among the smaller iron particles allow them to move with greater freedom, leading to a mechanism known as three-body abrasion. In this process, the abrasive particles have the freedom to roll on the interacting surface due to the reduced magnetic forces among them.

CHAPTER 5: SUMMARY AND FUTURE WORK

This dissertation presents several areas of magnetic-field assisted finishing (MAF) that can be further explored and improved. The first part of the study focuses on optimizing the processing parameters on mold steels and sheet metal through extensive experiments and fractional factorial design (FFD). The optimal processing parameters were determined by statistically analyzing the interplay of all processing parameters via fractional factorial design and DOE analysis. Subsequently, supplementary experiments were carried out to enhance the efficiency of the polishing process, commencing with a rough surface. The findings from both the comprehensive parameter analysis and the additional experiments were utilized to design a multi-step MAF process for the HP4M mold. Comparisons were made between the MAF performance and manual finishing, revealing final roughness values of 26 nm and 20 nm, respectively, starting from an initial surface roughness of 434 nm. Additional experiments were conducted on an AISI S7 steel workpiece to further validate the analytical approach, employing different processing parameters as these parameters were identified as more efficacious in prior studies. The optimized parameter settings significantly improved the final surface roughness, reducing it from 507 nm to 45 nm.

The MAF process was then utilized to polish sizable sheet metal samples coated with chrome. The objective was to identify the most favorable processing parameters. The investigation revealed that employing a stiffer brush with a higher weight ratio of ferromagnetic particles proved to be more effective in enhancing the MAF performance for finishing sheet metal samples. This conclusion was based on the analysis of surface characteristics measured using a profilometer. Below are potential future directions that can be extended from the findings discussed in the first part of the study:

- In the design of experiment (DOE) analysis for HP4M mold steel, only two sizes of abrasive (3 μm and 940 μm) were investigated using an FFD method. However, it is important to note that many other abrasive sizes should be considered in the DOE analysis. By examining only two extreme cases of this parameter, the analysis will only reveal the main effect represented by these two points. To gain a more comprehensive understanding and determine the optimum abrasive size, it is necessary to introduce additional abrasive sizes. This broader range of sizes will provide a more detailed representation of the graph, potentially resulting in non-linear curves rather than straight lines. Consequently, it will enable a more accurate determination of the optimal abrasive size for the given application.

- In order to optimize the processing efficiency of MAF, it is essential to include the processing time as a parameter in the Design of Experiments (DOE) analysis.
- Another aspect that should be explored is the influence of the weight or volume fraction of silicone oil on the viscosity and stiffness of the MAF brush. Currently, the experiment has involved two different weight fractions of silicone oil in MAF brush. However, a comprehensive study on the effect of stiffness necessitates varying the weight fraction of silicone oil, including cases where silicone oil is absent. This will enable a more thorough examination of the impact on the stiffness of the MAF brush, leading to a conclusive finding.

The second phase of the research built upon the previous study and specifically addressed the refinement of large sheet-metal surfaces. Initially, a small-scale setup was employed to establish the most favorable processing parameters for finishing chrome-coated metal sheet samples. These optimal parameters were identified, and they were then implemented in a continuous setup, enabling the successful completion of sheet metal samples with a larger surface area. By incorporating the optimized parameters into the continuous setup, the overall finishing process was significantly improved in terms of both effectiveness and efficiency. Further study based up this investigation can be as follows:

- Apply the large-scale setup on varieties of materials such as Ti-6Al-4V.
- Integrate this setup in different mechanical systems. The present work only integrated the continuous setup into the CNC mill. It is worth implementing the setup into a CNC lathe or robot arm system.

The last part of the study aimed to establish a systematic approach for determining the ideal processing conditions concerning abrasive particle size, iron particle size, and traversing passes in the MAF process. The research yielded valuable insights into optimizing the brush constituents to enhance process efficiency. To improve material removal and surface quality, it is recommended to utilize smaller BC and larger iron particle sizes. The study revealed that the optimal number of passes varied depending on the BC size. As the BC size decreased, the optimal passes occurred earlier, leading to an improved surface finish. Furthermore, Ansys simulations were performed to model the lateral interaction forces between large and small iron particles. These simulations aimed to explore how the size of iron particles affects the behavior of the brush components. It demonstrated that larger iron particles experience a more significant magnetic force, causing the

creation of sturdy chain-like formations and enhancing their ability to firmly grasp abrasive particles. This arrangement enables a two-body abrasion mechanism, thereby enhancing the processing capability. Conversely, smaller iron particles experience weaker magnetic forces between them through the simulation, allowing them to roll freely. This leads to a three-body abrasion mechanism during the MAF process. In addition to the presented study, the following improvements should be made in the future:

- The size range of the two main constituents (iron and BC) should be expanded to make a more improved and broad result.
- Examining the state of iron particles both before and after the MAF is significant. Given that the brush comprises iron and abrasive particles, it is inevitable that iron particles will undergo wear and abrasion during the finishing procedure. Any alterations in the shape or size of the iron particles will consequently affect their conditions. As a result, such changes might potentially impact the performance of MAF, thereby warranting a thorough investigation into the influence of these factors on MAF performance will be necessary.
- The current simulation focused on simplifying the analysis of iron particles of different sizes. However, it is important to consider multiple parameters related to the brush constituents for a more accurate outcome. To achieve a more practical simulation of the MAF brush, it is recommended to incorporate additional factors such as the presence of abrasives and the liquid medium. This will provide a more realistic representation and enhance the credibility of the simulation.
- The MAF process possesses a distinctive capability to adjust and conform its brush to the workpiece surface, making it a suitable technology for refining 3D freeform surfaces. Although the present study concentrated solely on flat samples, there is a need to investigate and analyze the potential of MAF for finishing 3D surfaces.

BIBLIOGRAPHY

[1] Shengqiang Yang and Wenhui Li. (2018). *Surface finishing theory and New Technology*. Berlin Heidelberg: Springer.

[2] Hideyuki Kanematsu and Dana M. Barry (2018). *Corrosion control and surface finishing environmentally friendly approaches*. Tokyo: Springer.

[3] SAE Media Group. (2019). *3 key benefits: Better corrosion resistance, fatigue life, and part integrity*.
Online:https://www.techbriefs.com/component/content/article/tb/stories/news/33042.

[4] D. Novovic, R.C. Dewes, D.K. Aspinwall, W. Voice, and P. Bowen. (2004). *The effect of machined topography and integrity on fatigue life*. International Journal of Machine Tools and Manufacture, 44(2-3):125–134. doi: 10.1016/j.ijmachtools.2003.10.018.

[5] R.G. Bayer and J.L. Sirico. *The influence of surface roughness on wear*. (1975). Wear, 35(2): 251–260. doi: 10.1016/0043-1648(75)90074-5.

[6] B Bhushan and Pak Lim Ko. (2003). *Introduction to tribology*. Applied Mechanics Reviews, 56 (1). doi: 10.1115/1.1523360.

[7] E.S. Gadelmawla, M.M. Koura, T.M.A. Maksoud, I.M. Elewa, and H.H. Soliman. (2002). *Roughness parameters*. Journal of Materials Processing Technology, 123(1):133–145,. doi: 10.1016/s0924-0136(02)00060-2.

[8] Keynence. *Arithmetical Mean Height (Ra, PA, WA): Surface Roughness Parameters. Arithmetical Mean Height (Ra, Pa, Wa), Surface Roughness Parameters, Introduction To Roughness.* KEYENCE America.

[9] UPMOLD. (2021). *Surface Finish RA and RZ Roughness Specification*. Upmold Technology Limited. upmold.com/surface-finish-ra-rz/.

[10] Fukuo Hashimoto, Hitomi Yamaguchi, Peter Krajnik, Konrad Wegener, Rahul Chaudhari, Hans-Werner Hoffmeister, and Friedrich Kuster. (2016). *Abrasive fine-finishing technology*. *CIRP Annals*, 65(2):597–620. doi: 10.1016/j.cirp.2016.06.003.

[11] W. B. Rowe. (2014). *Principles of modern grinding technology*. Elsevier/William Andrew. ISBN: 978-0-8155-2018-4

[12] M Kobayashi, T Matsui, and Y Murakami. *Mechanism of creation of compressive residual stress by shot peening*. (1998). International Journal of Fatigue, 20(5):351–357. doi: 10.1016/s0142-1123(98)00002-4.

[13] Anand C Petare and Neelesh Kumar Jain. *A critical review of past research and advances in abrasive flow finishing process*. (2018). The International Journal of Advanced Manufacturing Technology, 97(1-4):741–782. doi: 10.1007/s00170-018-1928-7.

[14] V K Jain, A Sidpara, M R Sankar, and M Das. Nano-finishing techniques: A review. *Proceedings of the Institution of Mechanical Engineers, Part C: Journal of Mechanical Engineering Science*, 226(2):327–346, 2011. doi: 10.1177/0954406211426948.

[15] E. J. Taylor and M. Inman. (2014) *Electrochemical surface finishing*. Interface magazine, 23 (3):57–61,. doi: 10.1149/2.f05143if.

[16] C.P. Ma, Y.C. Guan, and W. Zhou. (2017) *Laser polishing of additive manufactured Ti alloys*. Optics and Lasers in Engineering, 93:171–177. doi: 10.1016/j.optlaseng.2017.02. 005.

[17] ATH Beaucamp and Y Namba. Technological advances in super fine finishing. (2014) Proceedings of the 14th euspen International Conference, Dubrovnik, pages 1–19,.

[18] Rabinow, Jacob. (1948). *The Magnetic Fluid Clutch*. Electrical Engineering, vol. 67, no. 12, pp. 1167–1167, doi:10.1109/ee.1948.6444497.

[19] Pil-Ho Lee, Haseung Chung, Patrick Steven McCormick, Patrick Kwon, Hoa Nguyen, Yuhang Yang, and Chenhui Shao. (2018). *Experimental and statistical study on magnetic-field assisted finishing of mold steel using nano-scale solid lubricant and abrasive particles.* ASME 2018 13th International Manufacturing Science and Engineering Conference, Volume 3: Manufacturing Equipment and Systems,. doi: 10.1115/msec2018-6544.

[20] Manjesh Kumar, Hari Narayan Singh Yadav, Abhinav Kumar, and Manas Das. (2021). *An overview of magnetorheological polishing fluid applied in nano-finishing of components*. Journal of Micromanufacturing, page 82-100. doi: 10.1177/ 25165984211008173.

[21] H.B. Cheng, Yeung Yam, and Y.T. Wang. (2009). *Experimentation on mr fluid using a 2-axis wheel tool*. Journal of Materials Processing Technology, 209(12-13):5254–5261. doi: 10.1016/j.jmatprotec.2009.03.011.

[22] N A Mutalib, I Ismail, S M Soffie, and S N Aqida. (2019). *Magnetorheological finishing on metal surface: A review*. IOP Conference Series: Materials Science and Engineering, 469:012092,. doi: 10.1088/1757-899x/469/1/012092.

[23] Anant Kumar Singh, Sunil Jha, and Pulak M. Pandey. (2011). *Design and development of nanofinishing process for 3d surfaces using ball end mr finishing tool*. International Journal of Machine Tools and Manufacture, 51(2):142–151. doi: 10.1016/j.ijmachtools. 2010.10.002.

[24] Chunlin Miao, John C. Lambropoulos, Henry Romanofsky, Shai N. Shafrir, and Stephen D. Jacobs. (2009). *Contributions of nanodiamond abrasives and deionized water in magnetorheological finishing of aluminum oxynitriden*. SPIE Proceedings. doi: 10.1117/12.826453.

[25] Ajay Sidpara and V.K. Jain. (2012). *Nano–level finishing of single crystal silicon blank using magnetorheological finishing process*. Tribology International, 47:159–166. doi: 10.1016/j.triboint.2011.10.008.

[26] Aman Kumar, Zafar Alam, Dilshad Ahmad Khan, and Sunil Jha. (2018). *Nanofinishing of fdm-fabricated components using ball end magnetorheological finishing process*. Materials and Manufacturing Processes, 34(2):232–242. doi: 10.1080/10426914.2018. 1512136.

[27] G. Parameswari, V. K. Jain, J. Ramkumar, and Leeladhar Nagdeve. (2017). *Experimental investigations into nanofinishing of ti6al4v flat disc using magnetorheological finishing process*. The International Journal of Advanced Manufacturing Technology, 100(5-8): 1055–1065. doi: 10.1007/s00170-017-1191-3.

[28] Harsh Kansal, Anant Kumar Singh, and Vishwas Grover. (2018). *Magnetorheological nanofinishing of diamagnetic material using permanent magnets tool*. Precision Engineering, 51:30–39. doi: 10.1016/j.precisioneng.2017.07.003.

[29] Dilshad Ahmad Khan and Sunil Jha. (2017). *Selection of optimum polishing fluid composition for ball end magnetorheological finishing (BEMRF) of copper*. The International Journal of Advanced Manufacturing Technology, 100(5-8):1093–1103. doi: 10.1007/s00170017-1056-9.

[30] Jisheng Pan, Kun Zheng, Qiusheng Yan, Qixiang Zhang, and Jiabin Lu. (2020). *Optimization study on magnetorheological fluid components and process parameters of cluster magnetorheological finishing with dynamic magnetic field for sapphire substrates*. Smart Materials and Structures, 29(11):114009. doi: 10.1088/1361-665x/abb988.

[31] Dhirendra K. Singh, V.K. Jain, and V. Raghuram. (2004). *Parametric study of magnetic abrasive finishing process*. Journal of Materials Processing Technology, 149(1-3):22–29. doi: 10.1016/j.jmatprotec.2003.10.030.K. Saraswathamma, Sunil Jha, and P.V. Rao. (2015). *Experimental investigation into ball end magnetorheological finishing of silicon*. Precision Engineering, 42:218–223. doi: 10.1016/j.precisioneng.2015.05.003.

[32] Anant Kumar Singh, Sunil Jha, and Pulak M Pandey. (2012). *Parametric analysis of an improved ball end magnetorheological finishing process*. Proceedings of the Institution of Mechanical Engineers, Part B: Journal of Engineering Manufacture, 226(9):1550–1563. doi: 10.1177/0954405412453805.

[33] Chinu Kumari, Sanjay Kumar Chak, and Vamula Vijay Vani. (2020). *Experimental investigations and optimization of machining parameters for magneto-rheological abrasive honing process*. Materials and Manufacturing Processes, 35(14):1622–1630. doi: 10.1080/10426914.2020.1779938.

[34] Faiz Iqbal and Sunil Jha. (2018). *Experimental investigations into transient roughness reduction in ball-end magneto-rheological finishing process*. Materials and Manufacturing Processes, 34(2):224–231. doi: 10.1080/10426914.2018.1512131.

[35] Anwesa Barman and Manas Das. (2017). *Design and fabrication of a novel polishing tool for finishing freeform surfaces in magnetic field assisted finishing (MAF) process*. Precision Engineering, 49:61–68. doi: 10.1016/j.precisioneng.2017.01.010.

[36] Ajay Sidpara and V.K. Jain. (2013). *Analysis of forces on the freeform surface in magnetorheological fluid based finishing process*. International Journal of Machine Tools and Manufacture, 69:1–10. doi: 10.1016/j.ijmachtools.2013.02.004.

[37] Anant Kumar Singh, Sunil Jha, and Pulak M. Pandey. (2012). *Nanofinishing of a typical 3d ferromagnetic workpiece using ball end magnetorheological finishing process*. International Journal of Machine Tools and Manufacture, 63:21–31. doi: 10.1016/j.ijmachtools. 2012.07.002.

[38] Zafar Alam, Faiz Iqbal, Sivasankar Ganesan, and Sunil Jha. (2018). *Nanofinishing of 3d surfaces by automated five-axis cnc ball end magnetorheological finishing machine using customized controller*. The International Journal of Advanced Manufacturing Technology, 100(5-8):1031–1042. doi: 10.1007/s00170-017-1518-0.

[39] Hitomi Yamaguchi and Arthur A. Graziano. (2014). *Surface finishing of cobalt chromium alloy femoral knee components*. CIRP Annals, 63(1):309–312. doi: 10.1016/j.cirp.2014. 03.020.

[40] C.A. Griffiths, S.S. Dimov, E.B. Brousseau, and R.T. Hoyle. (2007). *The effects of tool surface quality in micro-injection molding*. Journal of Materials Processing Technology, 189 (1-3):418–427. doi: 10.1016/j.jmatprotec.2007.02.022.

[41] A.R. Jones and J.B. Hull. (1998). *Ultrasonic flow polishing*. Ultrasonics, 36(1-5):97–101. doi: 10.1016/s0041-624x(97)00147-9.

[42] Ping Hu, Ning Ma, Li-zhong Liu, and Yi-guo Zhu. (2012). *Theories, methods and numerical technology of sheet metal cold and hot forming*. Springer London. Springer Series in Advanced Manufacturing. doi: https://doi.org/10.1007/978-1-4471-4099-3

[43] Ashwin Polishetty, Guy Littlefair, and K. Praveen Kumar. (2014). *Machinability assessment of titanium alloy ti-6al-4v for biomedical applications*. Advanced Materials Research, 941-944:1985–1990. doi: 10.4028/www.scientific.net/amr.941-944.1985.

[44] R.R. Boyer. (1996). *An overview on the use of titanium in the aerospace industry*. Materials Science and Engineering: A, 213(1-2):103–114. doi: 10.1016/0921-5093(96)10233-1.

[45] D.A. Axinte, J. Kwong, and M.C. Kong. (2009). *Workpiece surface integrity of ti-6-4 heatresistant alloy when employing different polishing methods*. Journal of Materials Processing Technology, 209(4):1843–1852. doi: 10.1016/j.jmatprotec.2008.04.046.

[46] Y. B. Tian, Z. W. Zhong, and S. J. Tan. (2016). *Kinematic analysis and experimental investigation on vibratory finishing*. The International Journal of Advanced Manufacturing Technology, 86(9-12):3113–3121. doi: 10.1007/s00170-016-8378-x.

[47] Zenghua Fan, Yebing Tian, Zhiqiang Liu, Chen Shi, and Yugang Zhao. (2019). *Investigation of a novel finishing tool in magnetic field assisted finishing for titanium alloy ti-6al-4v*. Journal of Manufacturing Processes, 43A: 74-82. doi: 10.1016/j.jmapro.2019.05.007

[48] Anwesa Barman and Manas Das. (2018). *Nano-finishing of bio-titanium alloy to generate different surface morphologies by changing magnetorheological polishing fluid compositions*. Precision Engineering, 51:145–152, 2018. ISSN 0141-6359. doi: https://doi.org/10.1016/j.precisioneng.2017.08.003.

[49] Bibek Poudel, Pil-ho Lee, Guangchao Song, Hoa Nguyen, Kayoung Kim, Kyoungho Jung, Chenhui Shao, Patrick Kown & Haseung Chung. *Innovative Magnetic-Field Assisted Finishing (MAF) Using Nano-Scale Solid Lubricant: A Case Study on Mold Steel*. International Journal of Precision Engineering and Manufacturing-Green Technology, vol. 9, no. 6, 2021, pp. 1411–1426, doi:10.1007/s40684-021-00404-w.

[50] Sidpara, Ajay, and Vijay Kumar Jain. (2012). *Experimental Investigations into Surface Roughness and Yield Stress in Magnetorheological Fluid Based Nano-Finishing Process*. International Journal of Precision Engineering and Manufacturing, vol. 13, no. 6, pp. 855–860, doi:10.1007/s12541-012-0111-6.

[51] Chris Manloney, Pierre Lormeau, Paul Dumas. (2016). *Improving Low, Mid and High-Spatial Frequency Errors on Advanced Aspherical and Freeform Optics with MRF*. Proceedings of the SPIE. Volume 10009 doi:10.1117-12.2236034

[52] Raul E. Riveros, Hitomi Yamaguchi, Taylor Boggs, Ikuyuki Mitsuishi, Kazuhisa Mitsuda, Utako Takagi, Yuichiro Ezoe, Kensuke Ishizu, Teppei Moriyama. (2012). *Magnetic Field-Assisted Finishing of Silicon Microelectromechanical Systems Micropore X-Ray Optics*.

Journal of Manufacturing Science and Engineering, vol. 134, no. 5, 2012, doi:10.1115/1.4006967.

[53] Jessica E. DeGroote, Anne E. Marino. John P, Wilson, Amy L. Bishop, John C. Lambropoulos, and Stephen D. Jacobs. (2007). *Removal Rate Model for Magnetorheological Finishing of Glass*. Applied Optics, vol. 46, no. 32, 2007, p. 7927, doi:10.1364/ao.46.007927.

[54] Khan, Dilshad Ahmad, and Sunil Jha. (2017). *Synthesis of Polishing Fluid and Novel Approach for Nanofinishing of Copper Using Ball-End Magnetorheological Finishing Process*. Materials and Manufacturing Processes, vol. 33, no. 11, pp. 1150–1159, doi:10.1080/10426914.2017.1328112.

[55] Harsh Kansal, Anant Kumar Singh, Vishwas Grover. (2018). *Magnetorheological Nano-Finishing of Diamagnetic Material Using Permanent Magnets Tool*. Precision Engineering, vol. 51, pp. 30–39, doi:10.1016/j.precisioneng.2017.07.003.

[56] Zafar Alam, Dilshad Ahmad Khan, Sunil Jha. (2018). *MR Fluid-Based Novel Finishing Process for Nonplanar Copper Mirrors*. The International Journal of Advanced Manufacturing Technology, vol. 101, no. 1–4, pp. 995–1006, doi:10.1007/s00170-018-2998-2.

[57] Prateek Kala, Sumit Kumar, Pulal M. Pandey. (2013). *Polishing of Copper Alloy Using Double Disk Ultrasonic Assisted Magnetic Abrasive Polishing*. Materials and Manufacturing Processes, vol. 28, no. 2, pp. 200–206, doi:10.1080/10426914.2012.746704.

[58] Jain, VK, Singh, P, Kumar, P, Sidpara, A, Das, M, Suri, VK, & Balasubramaniam, R. (2009). *Some Investigations Into Magnetorheological Finishing (MRF) of Hard Materials*. Proceedings of the ASME 2009 International Manufacturing Science and Engineering Conference. ASME 2009 International Manufacturing Science and Engineering Conference, Volume 2. West Lafayette, Indiana, USA. pp. 261-270.

[59] Sidpara, Ajay, and Vijay Kumar Jain. (2011). *Effect of Fluid Composition on Nanofinishing of Single-Crystal Silicon by Magnetic Field-Assisted Finishing Process*. The International Journal of Advanced Manufacturing Technology. Volume 55, 243-252. doi: https://doi.org/10.1007/s00170-010-3032-5

[60] Jiang Guo, ZhiEn Eddie Tan, Ka Hing Au, Kui Liu. (2017). *Experimental investigation into the effect of abrasive and force conditions in magnetic field-assisted finishing*. The International Journal of Advanced Manufacturing Technology, Volume 90, 1881–1888 (2017). doi: https://doi.org/10.1007/s00170-016-9491-6

[61] Chung Wai Kum, Takashi Sato, Jiang Guo, Kui Liu, David Butler. (2018). *A Novel Media Properties-Based Material Removal Rate Model for Magnetic Field-Assisted Finishing*.

International Journal of Mechanical Sciences, vol. 141, pp. 189–197, doi:10.1016/j.ijmecsci.2018.04.006.

[62] Abdul Wahab Hashmi, Harlal Singh Mail, Anoj Meena, Irshad Ahamad Khilji, Chaitanya Reddy Chilakarmarry, Siti Nadiah Binti Mohd Saffe. (2022). *Experimental Investigation on Magnetorheological Finishing Process Parameters*. Materials Today: Proceedings, vol. 48 pp. 1892–1898, doi:10.1016/j.matpr.2021.09.355.

[63] Yamaguchi, Hitomi, and Takeo Shinmura. (2004). *Internal Finishing Process for Alumina Ceramic Components by a Magnetic Field Assisted Finishing Process*. Precision Engineering, vol. 28, no. 2, pp. 135–142, doi:10.1016/j.precisioneng.2003.07.001.